A methodical approach for the design of thermal energy storage systems in buildings: An eightstep methodology

Received: 29 October 2023 | Revised: 8 February 2024 | Accepted: 22 February 2024

DOI: 10.1002/est2.600

RESEARCH ARTICLE

ENERGY STORAGE WILEY

A methodical approach for the design of thermal energy storage systems in buildings: An eight-step methodology

Samira Rahnama[1] | **Mahmood Khatibi**[1] | **Alessandro Maccarini**[1] | **Mahmoud Murtala Farouq**[2] | **Parham Mirzaei Ahranjani**[3] | **Enrico Fabrizio**[4] | **Maria Ferrara**[4] | **Dragos-Ioan Bogatu**[5] | **Jun Shinoda**[5] | **Bjarne W. Olesen**[5] | **Ongun B. Kazanci**[5] | **Elaheh Bazdar**[6] | **Fuzhan Nasiri**[6] | **Chao Zeng**[7] | **Xu Wei**[7] | **Fariborz Haghighat**[6] | **Alireza Afshari**[1]

[1]Department of the Built Environment, Aalborg University Copenhagen, København, Denmark

[2]Architecture and Built Environment Department, University of Nottingham, Nottingham, UK

[3]Department of Civil and Architectural Engineering, Aarhus University, Aarhus, Denmark

[4]Department of Energy, Polytechnic of Turin, Turin, Italy

[5]Department of Environmental and Resource Engineering, International Centre for Indoor Environment and Energy(ICIEE), Technical University of Denmark, Kongens Lyngby, Denmark

[6]Department of Building, Civil and Environmental Engineering, Concordia University, Montreal, Quebec, Canada

[7]School of Mechanical Engineering, Southwest Jiaotong University, Chengdu, China

Correspondence
Samira Rahnama, Department of the Built Environment, Aalborg University Copenhagen, A. C. Meyers Vænge 15, 2450 København, Denmark.
Email: samira@build.aau.dk

Funding information
Energiteknologisk udviklings- og demonstrationsprogram

Abstract

Recent research focuses on optimal design of thermal energy storage (TES) systems for various plants and processes, using advanced optimization techniques. There is a wide range of TES technologies for diverse thermal applications, each with unique technical and economic characteristics. Matching an application with the most suitable TES system remains challenging. This study proposes an eight-step design methodology guiding the process from describing the thermal process to defining the most appropriate TES based on constraints and requirements. The steps include specifying the thermal process, system design parameters, storage characteristics, integration parameters, key performance indicators, optimization method, tools, and design robustness. Seven already-designed TES systems are evaluated to assess the methodology's effectiveness, where the design procedures have been adapted to the proposed steps. Case studies involve various applications with both sensible and latent TES systems, demonstrating the applicability of the proposed design procedure. A significant diversity exists among the design cases regarding the design objective, input, design, and output parameters. Nevertheless, the design procedure in each case can be deconstructed into the outlined design steps. The last design step has been excluded from all case studies due to insufficient

information regarding the robustness of the design process. The paper demonstrates how a methodical approach can be applied to examine the TES design and the integration. The design steps proposed in this study can serve as a foundation for developing a more systematic approach for designing TES systems in future works, resulting in simplifying the design process.

KEYWORDS

systematic design methodology, thermal energy storage design

1 | INTRODUCTION

Buildings contribute to 32% of the total global final energy consumption and 19% of all global greenhouse gas (GHG) emissions.[1] Most of this energy use and GHG emissions are related to the operation of heating and cooling systems,[2] which play a vital role in buildings as they maintain a satisfactory indoor climate for the occupants. One way to mitigate the environmental footprint of buildings is to integrate more renewable energy sources into their heating and cooling systems. However, renewable energy sources are often intermittent, creating a time delay between energy production and demand. For example, technologies like solar collectors exhibit productivity primarily during daylight hours, coinciding with the period of lowest domestic heating demand.

Thermal energy storage (TES) serves as a solution to reconcile the disparity between the availability of renewable resources and the actual energy demand. TES is a technology where thermal energy is stored by altering the internal energy of a material. This stored energy can then be utilized later for various heating and cooling purposes.[3] TES offers several benefits, including enhanced overall efficiency and increased reliability when integrated into an energy system. This integration results in lower investment and operating costs, along with reductions in GHG emissions.[4,5] As shown in Figure 1, TES technologies are typically classified in three categories: sensible, latent, and thermochemical.[6]

Sensible heat storage involves storing thermal energy by altering the temperature of the storage medium. In a latent heat storage system, heat is released or absorbed during phase changes within the storage medium. Finally, in thermochemical storage, thermal energy is stored and retrieved through the reversible breaking and reforming of molecular bonds in chemical reactions.[3] Each TES technology comes with its own set of advantages and disadvantages. While sensible TES is simple and widely demonstrated, it is limited by its relatively low energy storage density. On the other hand, thermochemical TES can reach high energy storage density, but this technology is still under development due to technical challenges.[7]

Extensive research is ongoing in the realm of TES for buildings and numerous review articles already published on the topic.[8,9] Incorporating TES into building systems can yield advantages such as enhanced energy efficiency, a greater share of renewable energy utilization, and reduction in peak loads. As shown in Figure 2, TES in buildings can be classified into two primary categories:

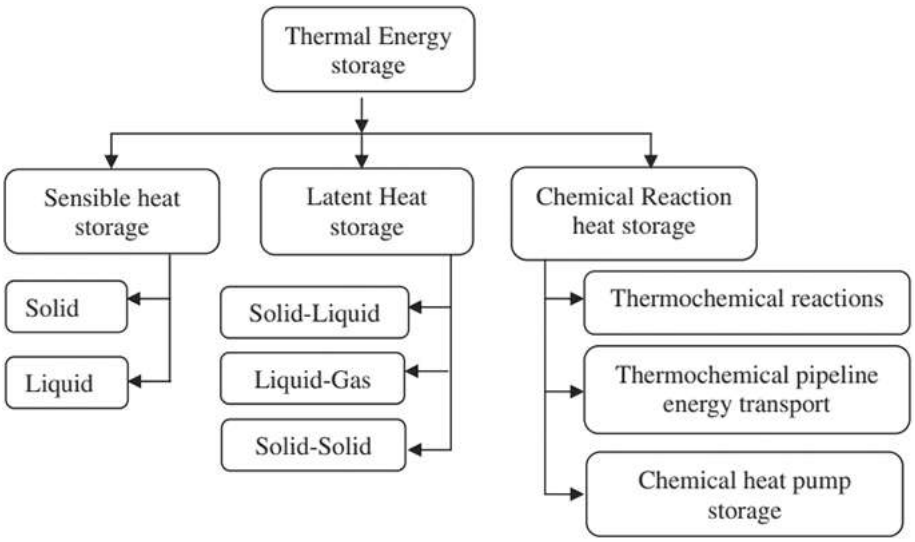

FIGURE 1 Classification of thermal storage technologies.[6]

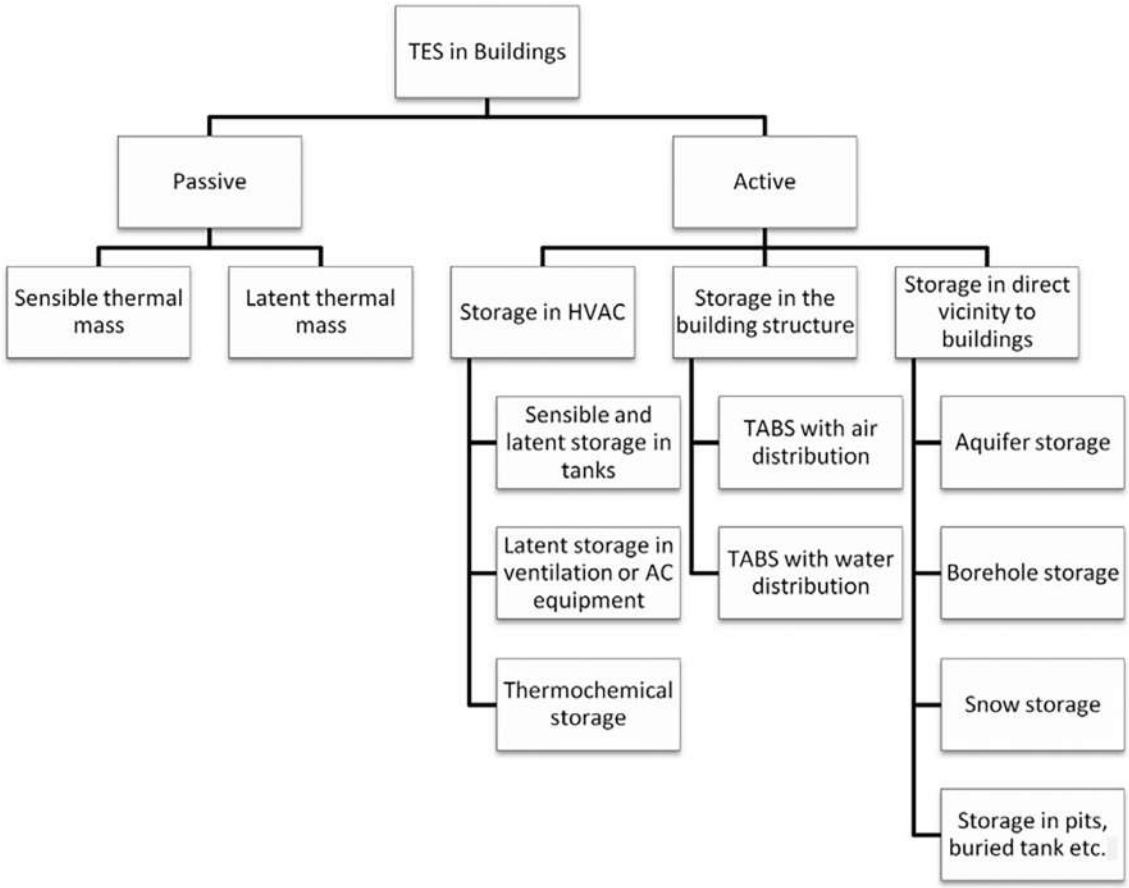

FIGURE 2 Classification of TES in buildings.[10] TES, thermal energy storage.

passive storage and active storage. Passive storage relies solely on the temperature difference between the storage system and its surroundings for charging and discharging. In contrast, active storage involves the assistance of pumps or fans for the charging and discharging processes.[10]

As shown in Figure 2, various technologies of TES systems with different thermal properties can be utilized in buildings. On the other hand, there are various types of building requiring the integration of TES systems for different purposes, for example, increasing energy efficiency or reducing energy costs and GHG emissions. Hence, an effective design of TES system, that is, choosing a proper TES technology with a proper size which meets the application-specific requirements can be a complex and challenging task and it depends on several factors. In a straightforward, conventional design, one can determine the storage system's size based on the worst-case scenario. However, this leads to an oversized estimation of the needed capacity. Optimal design of TES systems for various plants and processes using advanced optimization techniques is a subject of many recent research studies and has received considerable attention in the literature.

The optimal design of TES can be categorized based on the level at which the optimization occurs. Some of the studies only focus on the optimization of the storage design either at component level or at system level, whereas other studies also consider the optimization of the plant operation, where the storage system will be integrated. Depending on the level of design, there are different requirements that should be considered. For instance, in a study of Kuravi et al,[11] TES design considerations for a solar power plant at different levels have been reviewed. At the component level, the design emphasis is on the basic components of the TES, whereas at the system level, the integration of storage components with other systems, for example, pumps, heat exchanger (HEX) and control systems should be considered. The plant level design focuses on the plant requirements, for example, improving annual capacity factor of a solar power plant. When the integration of the TES into a plant is considered, the optimal design can be categorized according to the application, whether it is a retrofit application or a greenfield application.[12] The former examines the integration of the TES into a plant which already exists, whereas the latter is about the design of TES in parallel with the rest of the plant from the beginning of

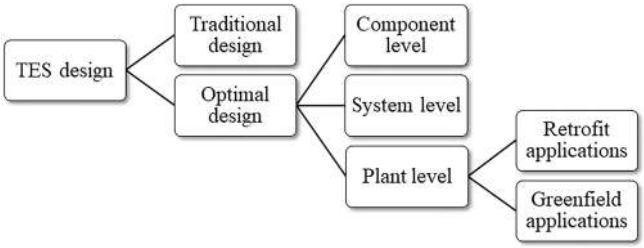

FIGURE 3 Classification of TES systems design. TES, thermal energy storage.

the plant design. Depending on whether it is a retrofit or a greenfield application, the optimal TES technology can be different for that application. For instance, TES systems integrated into the building structure such as walls, floors and ceilings might better fit with greenfield applications. Figure 3 shows a general classification of TES design methodology.

Looking at the literature of the past 20 years, phase change material (PCM) stands out as a widely used TES technology tailored for various applications. For instance, in a study back to 2004, a semi-empirical thermal model was developed that can be integrated into a commercial software package for design optimization of a hybrid heat sink TES with a PCM unit.[13] In recent studies, Li et al[14] proposed a multiobjective optimization approach for designing a PCM-based TES system, where the proposed approach was illustrated for optimizing a heating system for an outdoor swimming pool utilizing PCM storage. In another example,[15] where the emphasis is on system-level design optimization, an experimental study was conducted to explore the effects of inlet water temperature and flow rate on the design of a water-based active PCM storage. Through a parametric study, Rucevskis et al[16] introduced an optimal design for a PCM storage system that involves PCM units integrated with a capillary pipe system. This design was proposed for the purpose of space cooling in nearly zero-energy residential buildings. The study showed the crucial parameters influencing the cooling efficiency and energy consumption of the system include the thickness of the PCM layer, the quantity of parallel pipes, pipe diameter, duration of night cooling, inlet temperature of the cooling water, and water velocity. The study by Cui et al[17] explored the optimal design for an active cool PCM storage system integrated with heating, ventilation, and air conditioning systems. Employing a model-based design approach, this study optimized the storage capacity to maximize the cost-saving potential that can be achieved from peak load management and participation in demand response programs. The optimization in a study of Maleki et al[18] aimed to reduce the phase change time and maximize the stored energy in a finned latent heat TES system, where the design variables included the number of fins, the volume fraction of fins, and the dimensionless fin length within a Pareto optimal design scheme.

Integration of PCM with solar energy systems represents a promising approach for enhancing energy efficiency, improving energy storage capacity, and advancing the adoption of renewable energy technologies. Kalbande et al[19] evaluated a hybrid system using nano-enhanced PCM with a parabolic dish solar collector to store solar energy via PCM. Comparison with various nano-enhanced PCMs and pure paraffin wax revealed higher thermal conductivity and faster phase transformation in the nano-enhanced PCM, where the CuO- multi-walled carbon nanotube-based system demonstrated the greatest latent heat storage capacity. The experimented hybrid system exhibited a wide temperature range (60°C–-180°C), suitable for space heating. Further design factors included selecting materials for the parabolic dish collector and the thermal storage container in this study. In a study of Kalbande et al,[20] an oil-based TES system with solar collectors was designed, in which PCM was filled in the cavity of the oil-based thermal storage, aiming for temperature ranges exceeding 200°C. The integrated system used nitrate salt as a PCM to store latent heat and aluminum oxide (Al_2O_3) and soybean oil nanofluid serving as a heat transfer fluid (HTF). Coupled with a parabolic trough solar collector, PCM achieved maximum temperature of up to 220°C. Furthermore, PCM can be used with photovoltaic (PV) panels to increase system efficiency by regulating the temperature of PV panels. By maintaining the PV panel temperature within an optimal operating range, the efficiency of the solar cells can be maximized, leading to increased energy production and higher overall system efficiency. The research study by Nandanwar et al[21] investigated the use of PCM to enhance the electrical conversion efficiency of PV modules by controlling their surface temperature. Among four types of PCM-filled PV modules, calcium chloride hexahydrate-filled PV system showed the highest performance, that is, electrical efficiency improvement of 7.5% at a tilt angle of 90°.

Another common TES technology designed for many applications is the building-integrated TES systems, that is utilizing thermally massive building materials, such as masonry block walls or concrete slabs, either in a passive or an active design. In a two-series publication,[22,23] Bastien and Athienitis conducted a comparison of various design concepts for the passive incorporation of thermally massive elements in buildings. They also introduced a design methodology for determining the size of such storage systems in solariums and greenhouses. According to Bastien and Athienitis,[22] identifying the

design objective is the most important factor that should be considered in the first place when designing a passive TES system. Depending on the design objective, different materials and configurations can be appropriate, for example, massive exterior wall or direct-gain/isolated-gain space. In the initial phase of this study, various design objectives were examined, including minimizing indoor temperature fluctuations, decreasing energy consumption for space heating and cooling, and postponing the impact of peak solar gain. Subsequently, the study identified the most suitable design concepts for isolated-gain applications, considering factors such as the daily average operative temperature swing, as well as the minimum and maximum operative temperature. In the second series,[23] six distinct configurations of solariums were simulated using frequency response and finite difference thermal network modeling approaches. This investigation aimed to assess the influence of various design variables, such as the TES material or the variation in thermal resistance of the insulation layer, on the designated design objectives. Following a comprehensive analysis of simulation results, a design methodology consisting of 11 steps has been provided, together with recommendations to adopt the appropriate size of TES in different configurations and for satisfying different design objectives. In another study,[24] a design procedure has been provided for the active building-integrated TES systems that is, when passive elements embody a mechanical charging system such as hydronic systems for exchanging heat with the storage media.

As seen, a wide range of TES technologies are available that can be integrated into a variety of thermal applications. Each TES technology has its own technical and economic characteristics that make it more suitable for a specific application. Identifying important factors and then matching an application with the most appropriate TES system is still a challenging issue. A group of papers merely optimizes the thermal performance of TES systems.[25-28] However, the requirements for TES systems differ significantly depending on the chosen application. As a result, it is crucial to devise design methods that enable a TES system to meet the particular requirements of a given thermal application. In this context, a second group of papers optimizes the global performance of the application in which the TES system is integrated.[29-31] Nevertheless, a deep knowledge of the process under analysis is required for the second group and they depend on intricate simulations that are notably time-consuming. On the other hand, the increasing advancement of low-cost IoT devices and simulation tools together with data analysis techniques is expected to make the process modeling easier and faster at a reasonable cost and remove the barriers for complex simulations in near future. In addition, developing systematic assessment procedures for TES systems integrated into various applications can contribute to furthering their widespread implementation.[12]

Current barriers to commercial deployment of TES systems involve the intricate design process that must account for the peculiarities of both the TES system and the application under consideration. Indeed, there is a gap between the two approaches that should be filled by fast and easy to apply methodologies capable of aligning the thermal characteristics of a TES system with the requirements of the thermal application. The primary challenge is to create a set of methodologies to guide the process from description of the thermal process to defining TES geometry based on the requirements and constraints of thermal application.[32] Taking a broader view, TES systems are a part of a wider group of flexibility alternatives. Considering the growing number of factors which are increasing system complexity, there is still much room for the design of integrated energy systems, along with the advancement of streamlined building/district modeling tools and system optimization techniques. For example, adopting systematic approaches is essential to pinpoint the optimal combination of market signals and infrastructure. In this way, commercial models of TES operation as well as more efficient use cases can be developed.[33]

There are few studies which deal with systematic approaches in research studies regarding TES systems. For instance, Gibb et al[12] propose a systematic methodology consisting of three specific steps for characterizing and assessing TES systems in diverse applications. The main step in the proposed methodology involves analyzing the thermal process, which encompasses the structured gathering and examination of process data. In the next step, it is crucial to define the system boundary, delineating the interface between the fluid and the thermal sinks/sources, along with specifying the technical properties of the system. Finally, via determination of relevant key performance indicators (KPIs), the advantages that the TES system brings to the overall process are investigated. Two case study power plants, a concentrating solar plant and a cogeneration one, were evaluated using the proposed methodology in this research.

Particularly, when it comes to TES design, literature review reveals a lack of systematic approach for design and integration of TES systems into buildings. Considering different working principles of TES technologies, providing a systematic design approach that can be applicable to a variety of technologies and applications is not straightforward, however a consistent and systematic design methodology is crucial to appropriately compare technologies and design options. To our best knowledge, the only study which addresses this topic is the study conducted by Campos-Celador et al[32] They propose a

general methodology divided into four steps for the design of TES systems. During the first step, the thermal process needs to be characterized by its nominal parameters, such as the mass flow rate and temperature of the HTF. In the second step, design parameters are clearly defined. Likewise, a TES technology should be characterized in the third step that meets the specifications and constraints imposed by the first two steps. The final step is the determination of the TES design. The suggested methodology was applied to a domestic micro-cogeneration case study. As highlighted by the authors, the straightforward methodology introduced in their study can serve as a foundational step for the design of TES systems in the early phases of a project. However, it is recommended to conduct a more in-depth analysis, especially concerning the interaction between the TES and the application. Inspired by this research study, the presented methodology by Campos-Celador et al[32] is further developed in the current research study and then implemented on a few case studies. The present paper differs from published research studies on TES design by addressing a methodical approach for designing and integrating TES systems into buildings. While a previous study by Campos-Celador et al[32] has contributed to this area, they focus solely on system design parameters. Our research builds upon the methodology proposed by Campos-Celador et al[32] by incorporating both system design and integration parameters. The key contributions of the present study include:

1. Proposing a methodical approach for the design of TES systems which accounts for not only the system design parameters, but also the integration parameters. The proposed design methodology can serve as a foundation for developing a more systematic TES design and integration methodology.
2. Evaluating the proposed methodology with applying the proposed steps on seven different prior design case studies, all conducted by the authors.

The specific objective is to offer a more systematic approach to TES design and integration, hence simplifying the overall design process. The rest of this paper is organized as follows. The proposed design methodology is introduced in Section 2. In Section 3, the proposed design methodology is adapted to seven different already-designed TES systems. Finally, Section 4 is discussion and conclusion.

2 | METHODOLOGY

Figure 4 illustrates a flowchart of the suggested design methodology, providing examples of options for each step. The design methodology consists of the following eight steps:

Step 1: Specification of thermal supply and demand.
Step 2: Specification of TES system parameters.
Step 3: Specification of storage characteristics.
Step 4: Specification of integration parameters.
Step 5: Specification of KPIs.
Step 6: Specification of optimization method.
Step 7: Specification of optimization tools.
Step 8: Specification of robustness.

A fundamental input to the design process is the objective of design optimization. The choice of optimization objective is an important consideration that can have impact on the entire design process and the assessment of the TES design. In retrofit applications, the focus is on the requirements of an existing application, whereas greenfield applications can emphasize on all the benefits the storage can deliver to an application. Therefore, it may be possible to well identify the objective of the optimization in greenfield applications in advance, while this can be possible after comprehensive analysis of the process in retrofit applications.[12] The choice of optimization objective is important to identify the required inputs and specify the relevant system design parameters. For instance, for peak shaving design, collecting information on thermal demand peak conditions is necessary when the thermal process is characterized in the beginning of the design process, or the reaction time of the TES system is a relevant design parameter when the objective is to optimize ancillary services provision for grid-interactive TES systems.

Likewise, optimization objective is a decisive factor for choosing the most appropriate TES technology, for example, whether a passive or an active, a direct-contact or an indirect contact TES technology should be employed. Passive TES system can often be a choice when the objective is maximization of the thermal comfort or minimization of energy demand, whereas active TES can be more suitable for peak shaving objective. The charging and discharging time of indirect TES systems is generally slower when compared to direct TES systems.[34] Therefore, one of these technologies can be more suitable when the optimization objective implies some restrictions on the charging and discharging rate, either directly at the system-level optimization or indirectly at the plant-level optimization. As another example, when overall cost optimization is among the objectives, direct TES systems can be a better option in comparison to indirect ones. Finally, KPIs are established, aligning with the optimization objectives to evaluate the TES design and quantifying the degree to which a particular optimization goal is achieved.

Depending on the type of the application, whether it is a greenfield or a retrofit application, some limitations

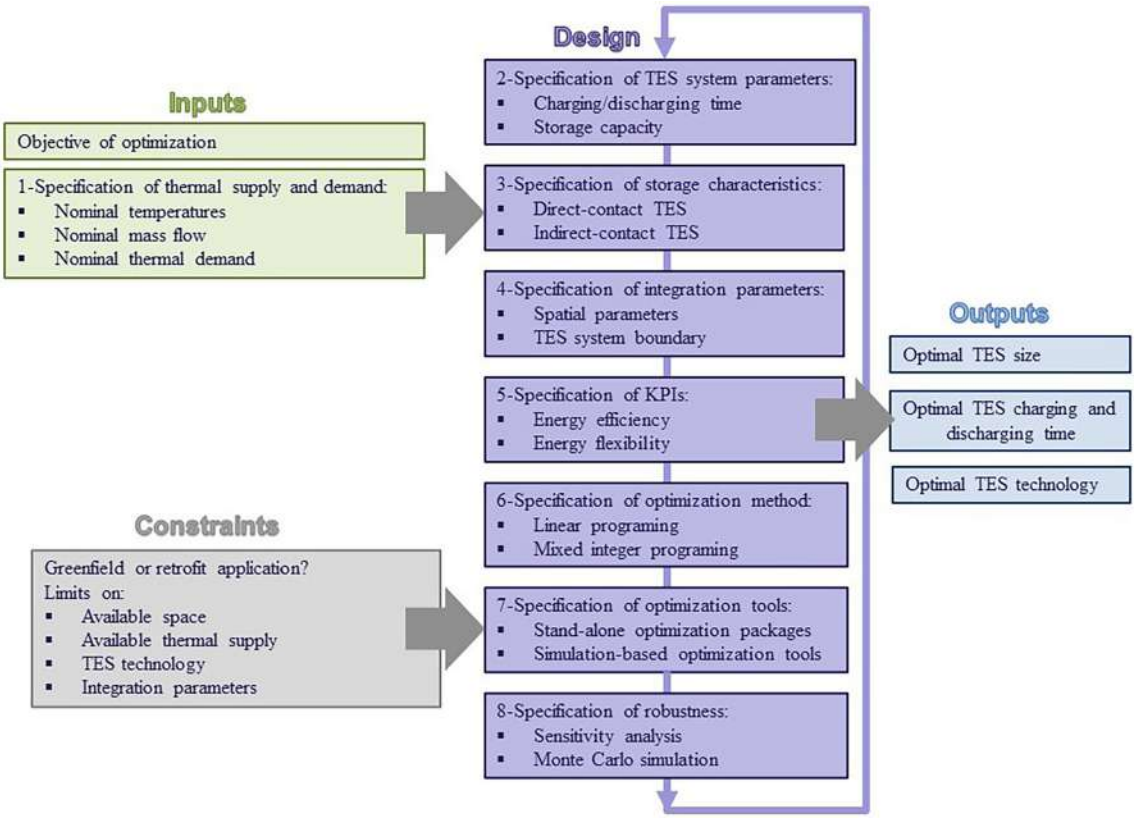

FIGURE 4 Flowchart of TES design methodology. TES, thermal energy storage.

may be imposed on the design methodology that should be defined beforehand. These limitations are considered as constraints for the design optimization. Generally speaking, retrofit applications are less flexible in terms of design parameters compared to greenfield applications, hence applying more constraints to the system design. For instance, there may be limitations on the available physical space for the storage system which can further limit the options for the storage technology.

Once all the design constraints are determined, the thermal process, including thermal supply and demand should be characterized in the first step of the design methodology. This step together with determination of the constraints and the objective of optimization provide the required inputs for the design procedure. Depending on the application, inputs may be a fixed value or a variable within a specific range, where the first group applies hard constraints, while the latter may apply soft constraints to the system design. The design methodology for a TES system is typically iterative in nature. The loop arrow is shown in the diagram to indicate the iterative procedure. The solution of the design optimization can be iteratively refined by adjusting the variable inputs in each iteration to optimize the relevant KPI. Typical outputs of the design process are the optimal TES size, charging and discharging time, and TES technology that can satisfy the application specific requirements. The following is the description of the design steps.

2.1 | Specification of the thermal supply and demand

Inputs to the proposed design methodology are the parameters which characterize the thermal process. To characterize a thermal process, three variables related to the HTF can be used: upper working temperature, lower working temperature and mass flow. In normal operation, the instantaneous values of such variables vary over time, and they typically oscillate around some nominal design values. Therefore, the following three nominal parameters, that is, nominal mass flow ($\dot{m}$), nominal lower temperature (T_{low}), and nominal upper temperature (T_{up}) can be used to characterize any thermal process. These parameters, along with the thermophysical properties of the HTF, can influence the selection of TES technology for a particular application.

In addition, in relation to interaction between the TES system and the application, nominal generation and demand should be given as input to the design methodology. The thermal demand and resource availability curves can be used to derive a few important parameters

for designing a TES system. The thermal demand and resource availability curves are prone to fluctuate, either seasonally or even on a day-to-day basis. For design purposes, it is crucial to have a single set of curves illustrating the thermal demand and resource availability. Designers can opt to utilize average conditions, reflecting the nominal behavior of the process, or they may choose to apply the most demanding conditions corresponding to the peak conditions of the TES system. The decision hinges on the integration objective behind the TES system and has a substantial impact on the anticipated benefits of TES integration.

2.2 | Specification of TES system parameters

The crucial design parameters for the TES system include:

- Charging time, indicating the available time duration for charging.
- Discharging time, denoting the available time duration for discharging.
- The storage capacity.

These design parameters can be extracted from the thermal demand and supply curves obtained in step 1. Likewise, desirable charging and discharging thermal power can be calculated using the above parameters.[32] According to the goal of the optimization, other parameters than above might be of interest that should be specified in this step. In Annex 30,[35] technical parameters for TES systems have been defined to facilitate comparison across TES technologies and applications. For instance, the minimum cycle length is defined as the shortest duration necessary for fully charging and discharging the system under nominal conditions. Alternatively, the response time is defined as the time interval between the issuance of a discharge request and the point at which the TES system attains its nominal power.

The design of heat storage systems is significantly influenced by both the temporal data resolution and the chosen evaluation timeframe. Temporal data resolution refers to the frequency at which data is collected (eg, minutely, hourly, monthly), while evaluation timeframe indicates the duration over which system performance is assessed (eg, a day, a month, a year). These factors impact system analysis, design, and effectiveness. Higher temporal resolutions, such as minutely or hourly data, provide detailed insights into fluctuations and patterns, enabling precise modeling and control. However, they might result in larger datasets and computational challenges. On the other hand, lower temporal resolutions, like daily or monthly data, offer broader views of trends but might miss out on short-term variations.

The choice of evaluation timeframe also has critical implications. Daily evaluations focus on short-term operational dynamics, while monthly evaluations capture larger trends and seasonal changes. Annual evaluations provide a comprehensive overview of system performance across different conditions. The decision on evaluation timeframe should align with the intended system goals and characteristics. For instance, residential energy storage might require daily evaluations to meet daily demands, while utility-scale systems might prioritize annual evaluations to accommodate seasonal variations. Striking the right balance between data resolution and evaluation timeframe is crucial for effective heat storage system design and accurate performance assessment.

2.3 | Specification of storage characteristics

TES systems are typically categorized based on the physical interaction between the storage medium and the HTF. Following this classification, TES systems can be divided into two main types: direct-contact TES systems and indirect-contact TES systems. In direct-contact TES systems, the HTF serves as the storage medium simultaneously. Conversely, indirect-contact TES systems incorporate a container or HEX that separates the storage medium from the HTF. One of the most common types of direct-contact TES is sensible heat TES, which employs water as the HTF, resembling the operational principle of storage tanks. In this scenario, the quantity of heat stored is contingent on factors such as the amount of storage material, the specific heat of the medium, and the temperature difference between the upper and lower nominal temperatures. The charging and discharging time corresponds to the duration required to fill or empty the tank's volume. Typically, a correction factor is introduced to account for the mixing effect.

In indirect-contact TES systems, the heat transfer relies on thermal processes occurring between the storage medium and the HTF. This contrasts with direct-contact TES, where heat transfer is based on mass transfer. The capacity of indirect-contact TES technology is typically characterized by the mean enthalpy variation of the storage medium, considering the sensible effect of the components involved in the thermal process. The time required for storing and releasing the heat in indirect-contact TES can be defined as a function of various operating parameters and design characteristics, including mass flow rate, nominal temperatures, and geometry.

Alternatively, some approaches in the literature introduce the concept of dimensionless time.

Direct-contact TES systems are generally cheaper and simpler in design as they involve fewer components. However, the choice of suitable materials for direct storage can be limited by factors such as stability and thermal properties. Indirect TES can be integrated with existing systems more easily, as the HTF can be chosen to match the requirements of the specific application. On the other hand, they tend to be more complex in design due to the need for additional components such as HEXs.

2.4 | Specification of integration parameters

Along with the design parameters, there are parameters associated with the incorporation of a TES system within the thermal process. For instance, spatial parameters such as available volume or available area address opportunities or problems regarding existing space, distances between process parts, obstacles, and available infrastructure. Moreover, the configuration of the TES system boundary is crucial in assessing TES integration. This boundary is defined as the interface between the thermal sink, thermal source, and the fluid streams. It encompasses all components, including HEXs, necessary for connecting the TES system to the overall process.

2.5 | Specification of KPIs

KPIs are measurable metrics used to assess the degree of success in achieving a particular optimization objective. A literature study reveals different categorizations of KPIs related to TES systems, for example, based on TES technology, that is, sensible, latent, or thermochemical[36] or based on assessment criteria, that is, technical, economic, or environmental KPIs.[37] Depending on the objective of optimization, KPIs can be defined at different technical levels, for example, component level, system level or plant level for TES integration.

Given the diverse range of applications for which TES systems can be integrated, the flexibility in defining KPIs is a crucial aspect. In this regard, Giacone and Mancò explored the need for a clear and systematic framework to identify the most pertinent KPIs for the integration of TES systems.[38] The identified KPIs can address a variety of criteria including energy efficiency, thermal comfort, reliability, cost, sustainability, and flexibility. Usually there is more than one KPI that should be optimized. Since these objectives are generally in conflict with each other, different technologies and configurations might be exploited. When designers are faced with such multiobjective optimization problems, a weighted average of KPIs is optimized as an objective function in some cases. However, previous knowledge of the system is required to select the weights. Also, tuning the weights is time-consuming. As a result, in some other studies, the Pareto approach, which results in a set of non-dominated solutions known as the Pareto frontier, is employed.

2.6 | Specification of optimization method

If the constraints and objective function of an optimization problem are a linear function of decision variables, it is called linear programing. Otherwise, the problem is called nonlinear programming. Mixed-integer linear programing is applied when there are binary or integer decision variables such as the status (on/off) of an equipment. Conventional deterministic gradient-based optimization methods, such as Newton, Quasi-Newton, and Steepest Descent, prove effective only for convex and smooth problems. Therefore, stochastic metaheuristic algorithms like Genetic Algorithm (GA) and Particle Swarm Optimization (PSO), which are population-based, are considered more efficient.

2.7 | Specification of optimization tools

Optimization tools can be categorized into two primary groups: stand-alone optimization packages and simulation-based optimization tools. Frequently mentioned stand-alone optimization packages in the literature include MATLAB, GenOpt, Topgui and modeFrontier. The two simulation-based optimization tools often mentioned in literature, aiming to integrate both optimization and simulation techniques, are Opt-E-Plus and BeOpt.

2.8 | Specification of robustness

It is essential to test the robustness of the system design to ensure its feasibility in real-word conditions, where the system is subject to uncertainties and disturbances. There are different tools and techniques for this purpose. For instance, sensitivity analysis is a widely recognized technique where the sensitivity function is computed as the ratio of the relative change in the output to the relative change in the input. This function is subsequently utilized to determine the impact of alterations in input parameters on the output of the system design. Another

well-known technique is the Monte Carlo simulation, in which the output of the system design is simulated given a range of random input variables to identify the probability of different outputs in a system design.

3 | CASE STUDIES

This section explains the design procedure of seven different already-designed TES systems based on the proposed design steps introduced in Section 2. No information was available regarding the robustness of the design; hence step 8 of the design procedure was omitted in all explanations.

3.1 | Earthbag-PCM integrated walls for temporary housings

Earthbag temporary housings are a viable solution to quickly accommodate a massive number of relocated people due to natural disasters, coercive movements, civil wars, insurgency, and so forth. These houses, nonetheless, face a poor indoor condition, especially in regions with harsh climatic conditions. To enhance their indoor condition, thus, the integration of PCM to the earthbag units is proposed as a potential technique. Hence, this study reports the development, modeling, and optimization of earthbag units for such applications. In this study, 24 earthbag unit blocks were fabricated to construct an earthbag test wall while each unit has a mixture of 30% clay and 70% well-graded soil sand.[39] The soil and the microencapsulated PCM (inertek26) and PCM composited were mixed at 2.2% of the composition of the entire unit block mixture. Water was added to the mixture up to the point where 10% moisture was achieved.[40]

- **Step 1:** To assess the behavior of PCM in an earthbag-building model, three identical real wall-scale prototypes were built, including Wall 1 (baseline) without PCM, Wall 2 with PCM encapsulated in expanded graphite and perlite (WA31) and Wall 3 with powdered PCM (WInk26). As shown in Figure 5, the prototype walls were then positioned within a climate-controlled thermal chamber to replicate the conditions of an indoor space in an earthbag building. The climate chamber was programmed to replicate summer climatic conditions in Kano, Nigeria. Additionally, k-type thermocouples (with a precision of 0.05°C) were situated on both the inner and outer surfaces of the test wall, and two heat flux sensors were installed on the wall to measure heat flow rates. Figure 5 displays a 3D sketch of the wall used for the simulation to validate the experimental work. The selection process took into account the comfort zone of Kano state, the designated region for the experiment, which was identified as ranging from 23°C to 32°C.[41]
- **Step 2:** A viable charging is the time at which the PCM is converted from solid to liquid when observing the energy during daylight with at least 70% of the daylight hours before completely converted to liquid and discharging is the time at which the PMC is converted from liquid to solid by releasing the stored energy with at least 70% of the night hours before completely converted into solid. This scenario can allow a complete phase change cycle within 24 hours of a day.
- **Step 3:** In a hot climate such as Nigeria, the PCM with a higher transition temperature option is preferable to reduce high temperatures.[42] The microencapsulated PCM and formed PCM composite had a phase transition temperature of 26°C and 31°C, respectively. The chosen PCM's heat storage capacities were 182 and 215 kJ/kg for A31 and Inertek26.
- **Step 4:** To meet the desired requirements for designing PCM-Earthbag walls, five parameters were considered, as presented in Table 1, such as the type and quantity of PCM material used, the size and shape of the bags, the wall dimensions, and the thickness of the insulation materials.
- **Step 5:** In this investigation, two principal performance measures were considered, including (1) the inner surface temperature reduction and (2) the viable PCM charging and discharging duration. The goal was to maximize the thermal comfort resulted from the earthbag unit walls.
- **Step 6:** In this study, GA is employed to optimize the average inner surface temperature of the earthbag building model. The objective is to determine the minimum average surface wall temperature that ensures the indoor environment of the earthbag model remains within the thermal comfort zone of Kano state, Nigeria (the chosen state for the experiment). The parameters considered include the earthbag wall thickness (EGT), building orientation (BO), PCM layer thickness (PLT). Hence, in order to enhance the efficiency of the earthbag-PCM units, a total of 230 distinct sets of simulation inputs were generated, encompassing variations in the independent operating variables. The resulting outputs from each simulation, specifically the average inner surface temperature, were utilized for a multivariable regression analysis.
- **Step 7:** In this study, the analysis of variance (ANOVA) equation developed through Excel data analysis serves as the objective function for GA optimization in MATLAB software. After establishing the

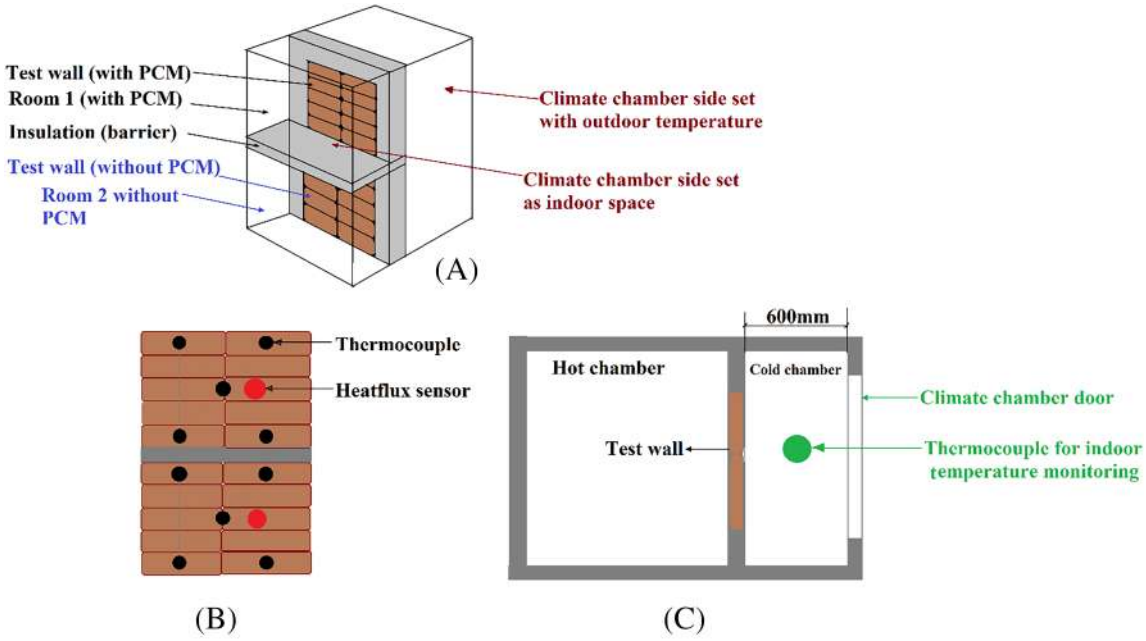

FIGURE 5 (Top) Physical arrangement of test wall prototype.

TABLE 1 Parameters and their properties.

Component	Thickness (m)	Area (m^2)	Number of block/walls	Quantity (kg)	Conductivity (W/m.K)	Density (kg/m^3)	Specific heat (J/kg.K)
Earthbag block	0.25	0.08	10	—	—	—	—
Earthbag wall	0.25	0.64	—	—	—	—	—
A31	0.03	—	—	2.2%w of EB*	0.2	680	2220
Inertek26	0.03	—	—	2.2%w of EB*	0.21	790	1071
Floor (EPS expanded perlite)	0.075	—	—	—	1.15	1900	950
Slab (EPS expanded perlite)	0.075	—	—	—	1.9	2300	1650

*Means 2.2% of total quantities of materials used in a single bag of earthbag unit block.

correlation between the independent variables, as explained earlier, GA is employed for optimization due to its effectiveness in addressing multivariable optimization problems. The objective is to minimize the variable "Average Inner surface temperature." Constraints related to the problem are imposed, with lower and upper limits for each variable provided in Table 2. GA parameters utilized in the optimization model are detailed in Table 3. Following this, the GA program is executed with the specified parameters and variable constraints. The optimized values of the variables are then extracted and presented in Table 4. Once the optimization was done with the GA as outlined, the optimized values listed in Table 4 were utilized to perform the final simulation with the EnergyPlus model. This simulation was then compared to the parametric analysis of the original design.

TABLE 2 Variable Bound for the key building design parameters.

S/N	Variables	Bound
1	Earthbag wall thickness (EGT)	200 mm ≤ EGT ≤ 450 mm
2	Building orientation(BO)	0° ≤ BO ≤ 90°
3	Phase change material layer thickness (PLT)	10 mm ≤ PLT ≤ 70 mm

3.1.1 | Results and conclusion on case study 3.1

The study's findings as shown in Table 5 demonstrate that introducing PCM into earthbag walls can lower surface temperatures by up to 1.92°C and 2.50°C for WA31 and WInk26, respectively. However, WInk26 with Inertek26 PCM proves ineffective due to surface temperatures consistently exceeding the PCM's melting point during the day, hampering charging and discharging cycles. On the other hand, A31 PCM exhibits a more favorable temperature profile, with a 19-hour charging and 3-hour discharging cycle, leading to its selection for further analysis. Parametric examination reveals that a 6 cm PCM layer with 16 hours of charging and 8 hours of discharging lowers the inner surface temperature of WA31 by 3.1°C. Interestingly, the optimized model suggests that optimal thermal comfort results can be achieved with just a 1-cm PCM layer. This optimized approach reduces the inner surface temperature by 5.82°C, demonstrating desirable outcomes for a 13-hour charging and 11-hour discharging cycle as shown in Table 6.

TABLE 3 Genetic Algorithm (GA) parameters for the present model.

S/N	GA parameters	Value
1	Population size	50
2	Number of iterations	100
3	Number of bits per variable	8
4	Crossover probability	0.8
5	Mutation probability	0.05

3.2 | The feasibility study and design optimization of a solar-assisted geothermal heat pump system for a real restaurant building in a mountain site

The system includes six thermal storages (see Figure 6 for its initial design configuration): three on the use-side storages (low temperature, high temperature, domestic hot water [DHW]) and three on the source-side storages (integration hot storage, Exhaust DHW storage, Ground for geothermal field). The design activity discussed here focuses on the three source-side storages, taking into account the overall seasonal demand for thermal energy determined through the dynamic simulation of the calibrated building model. The objective is to determine the optimal integration of these components to raise the temperature on the source side of the heat pump (HP) and enhance its coefficient of performance.[43]

- **Step 1:** Regarding the characterization of the thermal process, mass flow rates of the water acting as HTF were already fixed in the initial design considering the available circulating pumps of the different loops and the nominal flow rates expected at the source side of the HP. However, considering the unpredictable nature of the various heat sources supplying the different loops (exhaust DHW depends on the building use and the solar source is subject to weather conditions),

TABLE 4 Designed model and optimized values of the variable after analysis with GA and parametric analysis.

S/N	Variables	Designed model	Parametric analysis	Optimized value (GA)
1	Earthbag wall thickness (mm)	250	250	450
2	Building orientation (°)	0		90
3	PCM layer thickness (mm)	30	10-70	10

Abbreviations: GA, Genetic Algorithm; PCM, phase change material.

TABLE 5 Inner surface temperature reduction and charging and discharging results before optimization.

Earthbag wall	Temperature reduction (°C)	Charging (h)	Discharging (h)
WInk26_3 cm layer	1.92	24	0
WA31_3 cm layer	2.50	19	3
WA31_6 cm layer	3.1	16	8

Earthbag wall	Temperature reduction (°C)	Charging (h)	Discharging (h)
WA31_1 cm layer	5.82	13	11

TABLE 6 Optimized result for inner surface temperature reduction and charging and discharging.

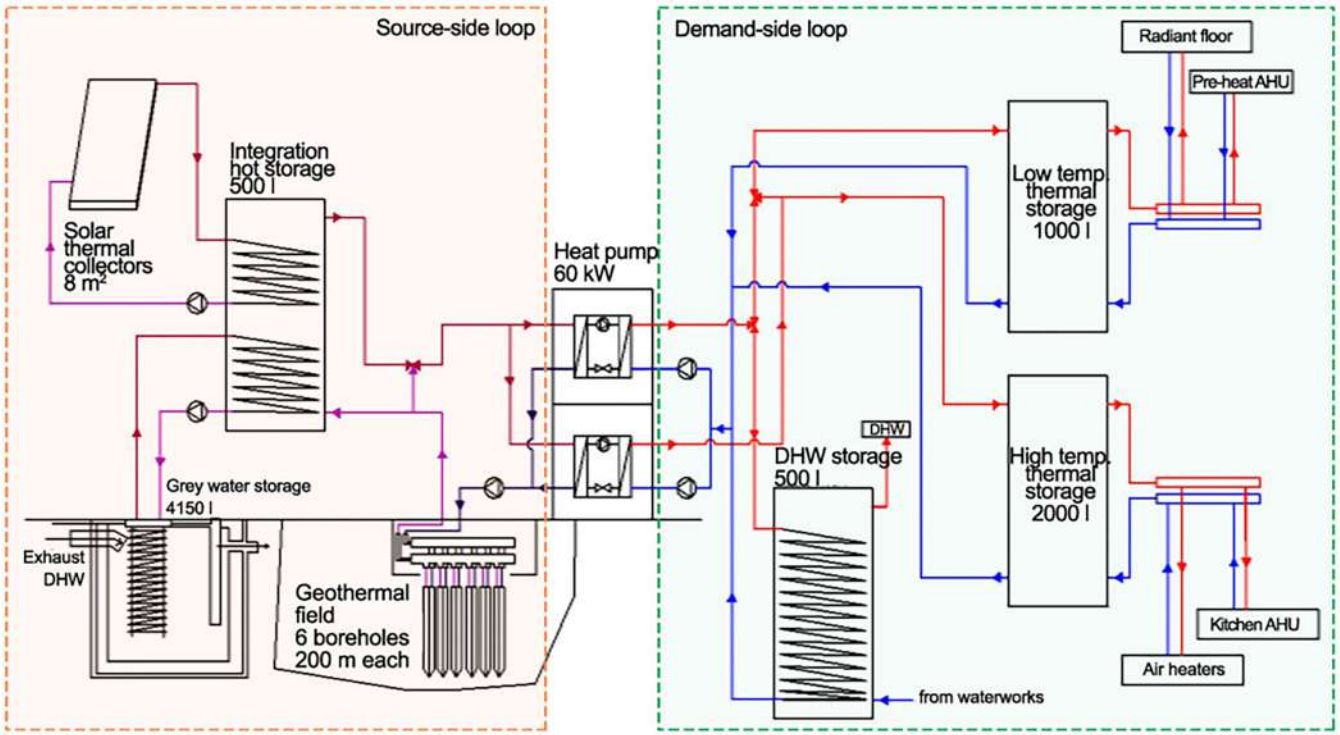

FIGURE 6 Schematics of demand side and supply side loops of the system.

the upper and lower working temperatures were not considered as inputs. Instead, they were treated as outputs of the design optimization activity. The appropriate constraints were set through control logics to ensure the automatic shutoff of a loop when temperature levels were too low to provide a positive contribution. The storage design in this case study relies on detailed thermal demand and resource availability curves derived from a detailed dynamic simulation calibrated on real monitored weather data at the building site. Rather than focusing on peak or average conditions, the design approach aims at exploiting such detailed dynamics looking for the TES optimal sizing and system integration that optimizes the seasonal performance of the overall system

- **Step 2:** Coherently with the characterization of the thermal process, the design parameters including the discharging as well as charging time, along with the related thermal power and storage capacity, were not fixed but were allowed to vary in relation to the variation of optimization parameters.
- **Step 3:** The project constraints dictated the specific storage technology to be employed in the system. One is the ground field, an indirect-contact TES that relates its storage capacity to the number and depth of boreholes, being the ground the storage medium and a water-glycole mix the HTF. The "gray water storage" is an underground water tank that is used as indirect-contact TES to store the heat recovered from exhaust DHW coming from the use-side, therefore relating its storage performance to its volume and the sizing of the HEX between the exhaust DHW (the storage medium) and the water circulating in the exchanger serpentine. The "integration hot storage" is a water tank storage acting as an indirect contact TES to integrate and store the heat coming from the three source loops (ground, solar, and gray water—if and when heat is available, with accurate controls). It is done by means of proper sizing of the storage itself and of the HEXs. For the two water tanks, water serves as the storage medium, and the HTF consists of water mixed with 40% glycol.
- **Step 4:** In this study, integration parameters were specified as optimization parameters, defined with a Min-Max variation range and discrete steps for variation in the range (Table 7). Regarding spatial integration parameters, the Min and Max volume of both Integration storage and DHW storages were set according to available space for installation of the tanks and the solar field, also considering detailed constraints regarding the min and max possible ratio between shows the optimal the water storage volume and the solar field (expressed in l/m^2). Also, the dimension of the ground storage, generated by the number and the depth of boreholes, was set according to available space for drilling in the project site. Regarding the TES system boundary parameters, the surfaces of the different HEX serpentines as points of contact between the different loops and the storages were used as design

TABLE 7 Optimization parameters.

	Name	Optimization parameter description	Unit	Min	Max	Step size
Spatial integration parameters	Ncoll	Number of solar thermal collectors	(−)	2	30	2
	Nbor	Number of geothermal boreholes	(−)	2	10	2
	Dbor	Depth of boreholes	(m)	50	350	25
	STVint	Volume of the Integration storage per solar collectors' area	(l/m^2)	40	100	10
	STVgw	Volume of the gray water storage	(l)	2000	8000	1000
TES system boundary parameters	Ssol	Surface of the solar heat exchanger serpentine in the integration storage	(m^2)	2.0	4.0	0.5
	Sgw, int	Surface of the gray water heat exchanger serpentine in the integration storage	(m^2)	3.0	7.0	0.5
	Sgw	Surface of the heat exchanger serpentine in the gray water storage	(m^2)	3.0	9.0	1

Abbreviation: TES, thermal energy storage.

parameters, given fixed flow rates of fluids circulating in the different loops.

- **Step 5:** According to the objective of the study, the defined KPIs refers to the system's comprehensive energy efficiency and cost-effectiveness. The cost-related KPI involves the total cost of the system over its estimated lifecycle (30 years), adhering to the formulation outlined in Standard EN 15459 for the economic evaluation of energy systems in buildings:

$$C_G(\tau,P) = CI + \sum_J \left[\sum_{i=1}^{\tau} (C_{a,i}(j) * R_d(i)) - V_{f,\tau}(j) \right] [€], \quad (1)$$

where $C_G(\tau,P)$ signifies the overall cost in relation to the initial year τ_0, considering a calculation period of τ years and the specified set of parameters P, CI denotes the initial investment cost, $C_{a,i}(j)$ represents the yearly cost for system component j at the year i (encompassing operational energy costs as well as expenses for routine or unexpected maintenance), $V_{f,\tau}(j)$ is the final value of component j at the end of the period τ and $R_d(i)$ is the discount rate applicable for year i.

The other KPI is the seasonal performance factor (SPF) of the system, which is defined, as applied in multipurpose systems,[44] as the ratio of the total useful energy output to the overall energy expenditure of a system as follows:

$$\mathrm{SPF_{SAGHP}} = \frac{Q_h + Q_v + Q_{\mathrm{DHW}}}{E_{\mathrm{el,HP}} + E_{\mathrm{el,aux}}} [-], \quad (2)$$

where Q_h, Q_v and Q_{DHW} are the useful energy outputs for ventilation, space heating and DHW, while $E_{\mathrm{el,HP}}$ and $E_{\mathrm{el,aux}}$ are the electrical energy inputs for the HP operation and the auxiliary systems (circulation pumps).

Considering these two objectives, the final KPI driving the optimization was defined as a multiobjective optimization function, expressed as follows:

$$\mathrm{MOF_{SAGHP}} = w_1 \frac{C_G - C_{G,\min}}{C_{G,\max} - C_{G,\min}} + w_2 \frac{\mathrm{SPF} - \mathrm{SPF_{max}}}{\mathrm{SPF_{min}} - \mathrm{SPF_{max}}} [-], \quad (3)$$

where $\mathrm{MOF_{SAGHP}} \in [0,1]$ and weights w_1 and w_2 were initially set to 0.5. After running single-objective optimization for both minimizing and maximizing the two objectives as inputs for Equation (3), the weights could be adjusted according to the investors' preference.

- **Steps 6:** To achieve the design objectives, a method employing simulation-based optimization was utilized. Given the discrete design space and the non-linearity of objective functions, the optimization runs were driven by the metaheuristic population-based PSO algorithm, selected in its binary version to deal with a discrete design space. The settings for PSO parameters were defined according to preliminary studies devoted to optimization of the algorithm performance in solving similar problems.[45]
- **Steps 7:** GenOpt software was used as optimization tool, with a tailored coupling to the detailed system dynamic model made in TRNSYS.

3.2.1 | Results and discussion on case study 3.2

From the system efficiency point of view, it is shown that the maximum attainable enhancement of the SPF

compared to the initial design is approximately 6%. However, this improvement comes with a potential substantial rise in the overall cost (+250%), primarily due to the high investment cost of boreholes. The adopted multiobjective optimization approach allowed identifying a solution that leads to nearly optimal SPF but significant containment of global cost (−34%), coherently with the investor's objective of maximizing the overall efficiency of the system with a view on global cost over the system lifecycle. In details, the higher cost-effectiveness resulted in the solar loop, whose size is maximized, while the heat recovery from exhausted DHW turned out to be less than anticipated, resulting in a reduction of its storage capacity. The planned number of boreholes resulted to be enough to increase the temperature level of the main loop by up to 5°C without causing unsustainable increase of global cost but, in order to avoid degradation of storage capacity of the ground field (resulting from multiyearly simulations of the overall system), in the summer period the solar system must be used for recharging the ground field.

3.3 | Macro-encapsulated ceiling panel with embedded pipes for water circulation

An active TES configuration similar to thermally active building systems (TABS) oriented to all new and retrofit building types was investigated at the Technical University of Denmark (DTU).[46] The PCM was macro-encapsulated in a ceiling panel with embedded pipes for water circulation, referred to as macro-encapsulated ceiling panel (MEP). The MEP, its operation, and water circuit are shown in Figure 7. Its construction ensured a direct contact between the PCM and the pipe profile. The MEP was designed to condition the indoor space during occupancy by absorbing the cooling load (passive operation). Active water circulation followed a rule-based control as a function of the operative temperature (top) during unoccupied hours, 18:00 to 08:00, discharging the PCM. However, the MEP could work as a radiant panel if needed during peak cooling loads. The piping structure was based on a commercially available product.

- **Step 1:** Water, that is, the HTF, is circulated through the pipes embedded in the PCM. Due to the MEP's configuration, the nominal mass flow rate was determined according to the TABS design procedure of ISO 11855-2:2015 and 11 855-3:2015.[46,47] The determined value relied on the specific heat capacity during the phase change, 242 Wh/m^2. The minimum and maximum water mass flow rates were 90 and 220 kg/h, respectively, to ensure a turbulent flow while avoiding noise.[47] The nominal upper temperature (T_{up}) of the water was selected according to the freezing temperature of the PCM, 21°C. The nominal lower temperature (T_{low}) should be selected to avoid any risk of condensation.[46,47] The total specific heat capacity of the panel was approximately 242 Wh/m^2 within the melting range.[46] The heat capacity of a single panel was ∼87 Wh,[46] with a total of 4144 Wh for the 48 panels included in the climatic chamber (Figure 7). This was because of the maximum usable ceiling coverage in the climatic chamber, which was ∼70% of the total floor area. Additionally, the volume of PCM per panel was limited by the load-bearing capacity of the suspended ceiling, aiming to prevent any potential leakage.[46]
- **Step 2:** The charging time represented the total occupancy time, 10 hours (from 08:00 to 18:00), since the cooling load was almost equal to the total heat capacity of the PCM ceiling. The discharge time could take place over the entire unoccupied period, which was 14 hours during the experiments (from 18:00 to 08:00).[46] For a supply water temperature of 20°C, the discharge time was 11 hours with the design water flow rate of 140 kg/h and approximately 7 hours with the maximum water flow rate of 220 kg/h. For a supply temperature of 18°C and a design water flow rate of 128 kg/h the discharge time was reduced to 6 hours.[47] Thus, the required time duration for the storage and release of heat can be determined as a function of the operational parameters and design features, specifically the cooling load, mass flow rate, and supply/return temperatures.
- **Step 3:** The MEP represents an indirect-contact TES prototype. The latent heat storage material was a solid-liquid PCM, paraffin, with a peak melting temperature of 24°C and a phase change range between 21°C and 25°C. The selection of the PCM was made in accordance with the specified comfort limits, 20°C and 26°C.[46,47]
- **Step 4:** The MEP was designed as a ceiling panel with 0.6 × 0.6 × 0.03 m^3 ($W \times L \times H$) dimensions, being easily integrated in regular suspended ceiling openings in Europe. Due to its design, radiant ceiling panels with PCM, the thermal storage is located next to the demand, that is, in the occupied space. With a PCM thickness of 0.01, the volume of material per panel was 3.6 dm^3 (∼3 kg per panel). Therefore, the maximum number of panels can be selected as a function of the cooling demand and the available ceiling area, for example, total minus the area required for lighting fixture, fire safety, and ventilation diffusers. In the climatic chamber, the panels were connected to a HEX through a closed loop. At the other end, the HEX was connected to a chiller (cooling source).

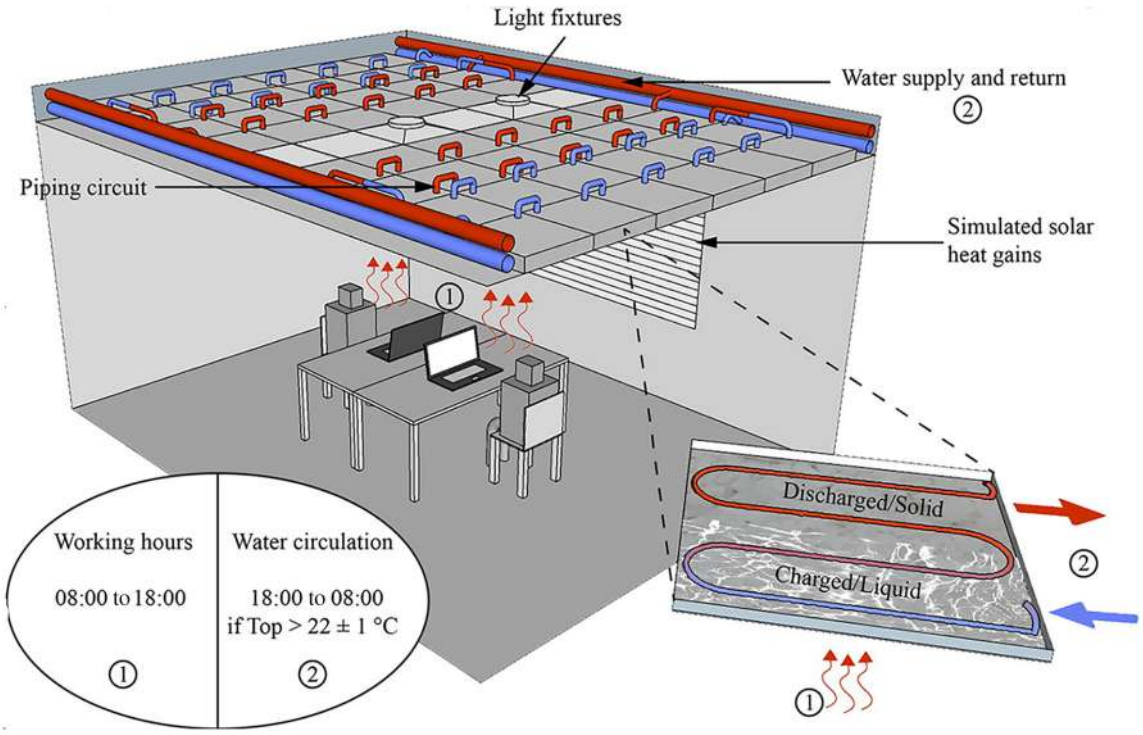

FIGURE 7 MEP panel operation principle.[46] MEP, macro-encapsulated ceiling panel; T_{op}, operative temperature.

- **Step 5:** The MEP was assessed in terms of energy efficiency, cost, thermal comfort, and flexibility. In terms of energy, the KPIs used were the specific cooling power during passive charging and active discharging and the primary energy use. Thermal comfort was assessed based on the indoor temperature range (eg, operative temperature) and temperature stratification (vertical temperature difference). For flexibility, the MEP's cooling load shifting ability but also supply water temperature range were investigated. Both global cost and payback period were used as KPIs for the economic analysis.
- **Step 6:** A parametric analysis was conducted for a building simulation model equipped with PCM panels to analyze the discharge method and to enhance the control and operation of the system. An optimization of different operating conditions and panel properties on the discharge of PCM ceiling panels was made.[47,48] Both water circulation and ventilation were investigated as discharge methods. The parameters investigated were the thermal conductivity of the PCM, air flow rate (night ventilation), water flow rate, water circulation schedule, and water supply temperature.[48] The supply water temperature and flow rate were further analyzed in the climatic chamber.[46,47]
- **Step 7:** The MEP was investigated in climatic chamber experiments[46] and building performance simulations in TRNSYS.[48,49]

3.3.1 | Results and discussion on case study 3.3

The panel registered during the experiments a specific cooling power between 5 and 28 W/m^2, with 11 W/m^2 on average during passive charging, that is, during occupancy. The thermal environment was maintained for 83% of the occupied time in category II of EN 16798-1:2019.[50] The temperature stratification was within the category A of ISO 7730 limits, with a temperature difference between head and ankles (1.1 and 0.1 m, respectively) of a seated occupant lower than 2 K.[46] The tests confirmed the MEP's load shifting ability, demonstrating its capacity to shift the cooling load from occupied to off-peak (unoccupied) hours.[46] Moreover, the panel presented high flexibility during discharge due to the wide range of water supply temperatures, 15°C to 21°C. This characteristic renders it compatible with a diverse range of renewable energy sources.[46,48]

A building simulation analysis of a recently renovated room at DTU compared the PCM ceiling panel to a TABS and all-air system in terms of energy, cost, and thermal comfort. The thermal environment and primary energy use were similar to TABS. The thermal environment was slightly worse than in the experiments, however with operative temperatures within 22°C and 27°C for more than 90% of the occupied time. The PCM ceiling panel registered a primary energy use similar to TABS,

16 kWh/m^2, 18% lower than the all-air system for the cooling season of Copenhagen, Denmark.[49] Additionally, both PCM and TABS registered a 30% reduction in the peak cooling power compared to the all-air system.[49] From a cost perspective, the global cost and payback period were calculated and compared to the results obtained from a TABS and an all-air system. In its current state it was determined that the MEPs were only slightly pricier than the all-air system under high cooling loads with a 20-year payback period, whereas TABS exhibited the lowest cost.[51]

With respect to discharging method, results showed that water circulation was a better discharging method than night ventilation since it increased the solidification percentage of the PCM. Enhancements in heat conductivity, extended water circulation operation time, and reduced supply water temperature contributed to the improved indoor thermal environment.[47] The increase in flow rate also benefitted the thermal environment as long as the water flow regime was turbulent, however, having a smaller effect than the other parameters analyzed.[47] When investigating the control strategy, it was determined that a control dependent on the operative temperature to reduce overcooling would benefit the thermal environment.[47,48]

3.4 | Sizing-designing approach for adiabatic-compressed air energy storage system toward self-sufficient building

In a conventional compressed air energy storage (CAES) system, known as diabatic-CAES (D-CAES), the thermal energy is lost during the compression process while the heat required for the expansion process is supplied by burning fossil fuel, particularly natural gas.[52] Adopting TES is a successful way to improve the D-CAES system efficiency while mitigating carbon emissions (CEs). Consequently, the second generation of CAES technology called adiabatic-CAES (A-CAES) emerged. In the A-CAES system, the produced heat during compression phase is captured and stored within a TES system and reused to heat the high-pressure air prior to the expansion phase. Hence, the A-CAES system can obtain up to 70% system efficiency while achieving a zero-emission system (no need to burn fossil fuels).[53] Figure 8 illustrates an A-CAES in an integrated energy system. As shown, the A-CAES system can contribute to the electricity, heating, and cooling network. Recently, Bazdar et al[54] studied the effect of a low-temperature double hot/cold tank TES system capacity on the performance of a grid-connected with a PV/ A-CAES system designed to meet the demand of an educational building located in Montreal-Canada. They proposed a sizing-designing methodology based on the long-term transient operation of an A-CAES system within an integrated energy system to meet the application-specific requirements considering techno-economic and environmental aspects.[55]

- **Step 1:** The hot and cold tank temperatures (Tup and Tlow) are set at 120°C and 25°C, respectively. While undergoing the charging phase, the heat generated in the compression stage is removed from high-temperature compressed air by HTF (eg, water) from the cold tank while passing through the cooling HEXs with an effectiveness of 95%. Then, thermal energy in the form of high-temperature HTF is stored in the hot tank and reused for heating the high-pressure air released from the air storage tank (at 25°C) before the expansion process (with an inlet temperature of 100°C) during the discharging phase. Figure 9 presents flowcharts of the proposed optimal design approach for an A-CAES integrated with TES and renewable energy systems. This strategy can be applied to different renewable energy resources, hybrid energy systems in different modes (eg, grid-connected, off-grid, stand-alone) and for various applications (eg, building, district, rural area, urban area, etc.). The TES-related outcomes is expected to be an optimum capacity and charging/discharging time for the TES corresponding to the size of solar power generation, CAES components (eg, compressor/turbine train, air storage tank), and building load demand. In this study, the building has an average hourly electricity demand of 645 kWh.
- **Step 2:** For the studied building to achieve a maximum 50% self-sufficiency, a 570 kW A-CAES system, including TES with a capacity of 3000 kWh (27 m^3) and charging (tc)/discharging (td) time of 5.12/3.78 hours, is needed.
- **Step 3:** The regenerative heat system includes two groups of cooling/heating counter-current HEXs and a direct-contact sensible TES with double hot and cold-water tanks.
- **Step 4:** A maximum of 12 961 PV panels (300 W each) can be installed based on the available rooftop area of the case study.
- **Step 5:** Depending on the user requirement and the system mode, various KPIs could be defined concerning the technical (eg, reliability, self-sufficiency, self-consumption, etc.), economical (eg, net present cost, cost of energy, profit, etc.), and environmental factors (eg, CE). To examine how the inclusion of the TES system in CAES influences the optimal configuration, and the KPIs, two scenarios corresponding to the different CAES configurations, such as D-CAES (with combustion chamber) and A-CAES (with TES), were

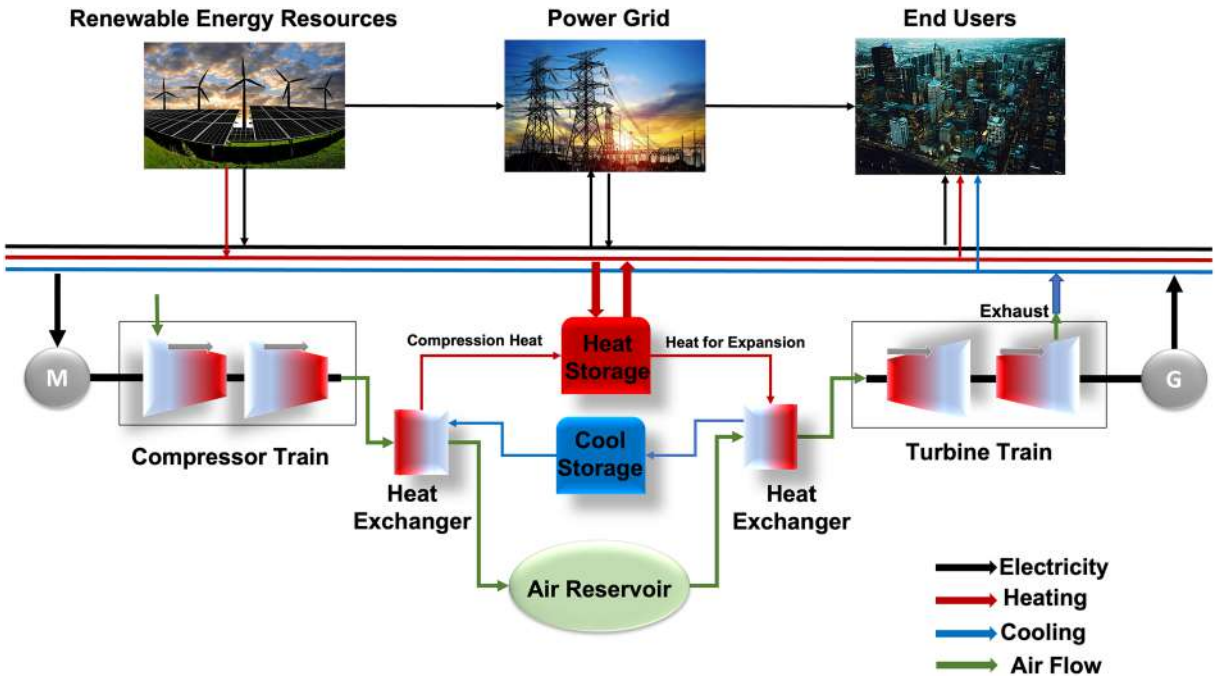

FIGURE 8 A-CAES with TES in the integrated energy system. A-CAES, adiabatic-compressed air energy storage; TES, thermal energy storage.

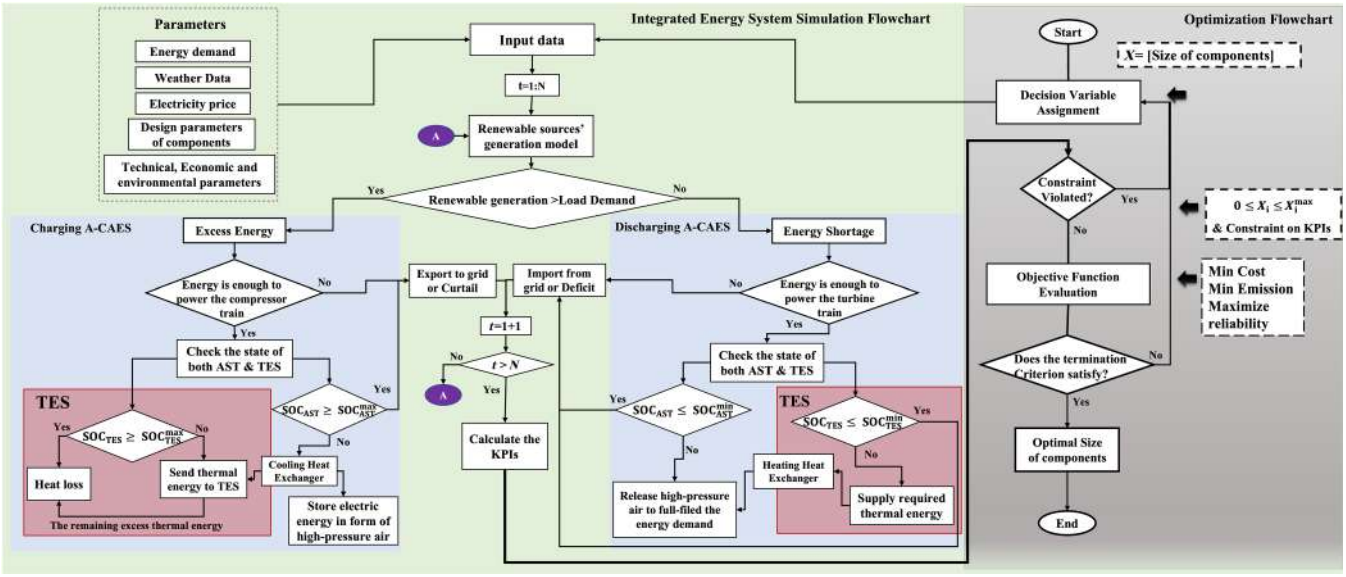

FIGURE 9 The designing flowchart for integrated energy systems, including renewables and A-CAES with TES. A-CAES, adiabatic-compressed air energy storage; TES, thermal energy storage.

investigated. Table 8 shows the optimal configurations and KPIs of proposed systems designed for electrification of one of the high-energy intensive buildings of Concordia university located in downtown of Montreal-Canada with an average hourly electricity demand of 645 kWh.

- **Step 6:** Given the economic model of each component in the integrated energy system along with the system's analytical model as a function of decision variables (components' design parameters), a mixed-integer nonlinear programming optimization problem can be formulated. The optimization problem aims to minimize the levelized cost of energy (LCOE) while achieving maximum building self-sufficiency ratio (SSR). The PSO method (with #20 particles and #100 iterations) was applied to solve the optimization problem for annual system operation with a 1-hour resolution.

TABLE 8 Optimal results of sizing D-CAES and A-CAES with TES system to meet the electric demand of an educational building in Montreal, Canada.

	Optimal configuration					KPIs' Value				
Scenario	Compressor (kW)	Turbine (kW)	AST (m^3)	TES (kWh)	P_{AST}^{Max} (MPa)	LCOE ($/kWh)	SSR (%)	HRR (%)	RTE (%)	CE (t/y)
A-CAES	585	526	300	3000	10.6	0.084	50	94	51.0	0
D-CAES	286	587	300	0	6.35	0.076	50	0	40.8	161

Abbreviations: A-CAEA, adiabatic-compressed air energy storage; CE, carbon emission; D-CAEA, diabatic-compressed air energy storage; HRR, heat recovery ratio; LCOE, levelized cost of energy; KPIs, key performance indicators; RTE, round-trip efficiency; SSR, self-sufficiency ratio; TES, thermal energy storage.

- **Step 7:** The simulation-optimization model was implemented in MATLAB software (version R2022a) running on an Intel Core i7-7500U CPU @ 2.7 GHz.

3.4.1 | Results and discussion on case study 3.4

As shown in Table 8, although PV/D-CAES has less LCOE of 0.076 $/kWh compared to 0.084 $/kWh for the PV/A-CAES system, thermal energy generated during the compression process recovered by around 94% in A-CAES leading to a zero-emission hybrid system compared to the PV/D-CAES with 161 t/year CE. Figure 10 shows the 1-year operation of TES in the studied hybrid PV/A-CAES system.

3.5 | Utilization of latent heat thermal energy storage (LHTES) integrated with geothermal energy system in underground engineering

TES systems utilizing PCMs are employed for peak load shifting in buildings. Enhancing the system's performance can be effectively achieved by burying it in the soil, capitalizing on the soil's high thermal inertia. In this case, Zeng et al[56] first proposed a model for an underground water tank incorporating PCM panels as thermal accumulators for a HP system. The buried water-PCM tank functions as a TES system coupled with a ground source HP (GSHP) for load shifting within an underground shelter. The thermal inertia of the geothermal energy is harnessed to maintain the PCM in a solid state initially and subsequently to naturally cool the tank once the PCM undergoes melting. The fluid is heat exchanged with the soil and the phase change plates through the phase change water tank, as shown in Figure 11.

- **Step 1:** Two operational strategies are provided based on the conditions of the underground shelter during normal circumstances (model 1) and emergency situations (model 2).
  - Model 1: The geothermal heat exchanger (GHE) offers heating and cooling to the underground shelters in normal mode. Based on the peak load, the maximum length of the GHE is determined.
  - Model 2: When compared to Model 1, the cooling load in the emergency mode exhibits a considerable rise. Parallel cooling is provided by the two halves, GHE and multimodular water-PCM tanks (MMWPT). By adding to and scaling MMWPT, the peak load difference between models 1 and 2 is eliminated
- **Step 2:** The PCM's thermal conductivity, the size and shape of the PCM panels, and the HTF's velocity in the spaces between the panels are the factors influencing the tank's performance. As shown in Figure 12A, water tanks are deigned to be connected in an $N \times M$ matrix shape, where M is the number of tanks in parallel and N is the number of tanks connected in series. A specific configuration of PCM panels in the MMWPT is shown in Figure 12B. The dimensions of water-PCM tank are 2000 mm in length, 600 mm in width, and 2000 mm in height. Inside the tank, there are PCM panels that are 1800 mm long, 60 mm wide, and 2000 mm tall. The phase change plates are spaced 20 mm apart.
- **Step 3:** Prior research has focused on achieving a specified load shifting through a single water-PCM tank, with its volume tailored to meet the necessary cooling or heating load. Zeng et al's[57] proposal for thermal storage in the underground shelter's emergency mode also includes MMWPT, which offers flexibility and is simple to mass-produce. The PCM is first kept in a solid form by geothermal energy, and the tank is naturally cooled after the PCM has melted.
- **Step 4:** The geothermal heat pump system (GHPS) is connected in series with MMWPT to provide cooling for the underground shelter in regular and emergency

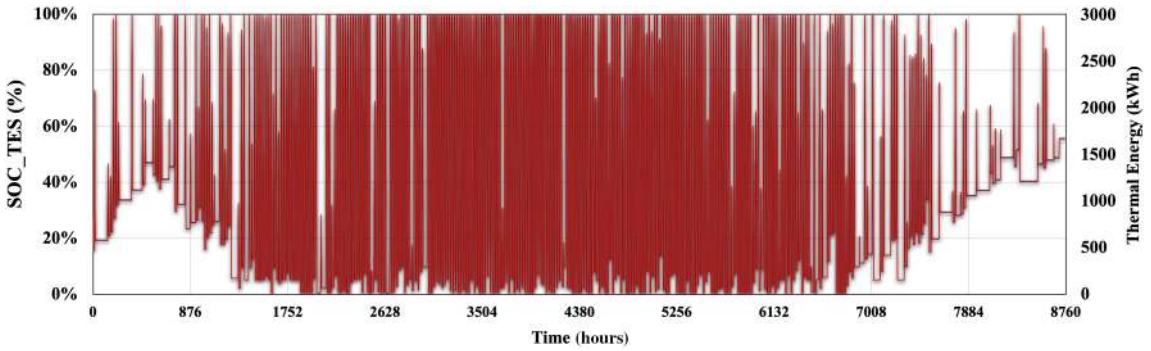

FIGURE 10 TES system dynamic behavior in the hybrid PV/A-CAES system over a year.

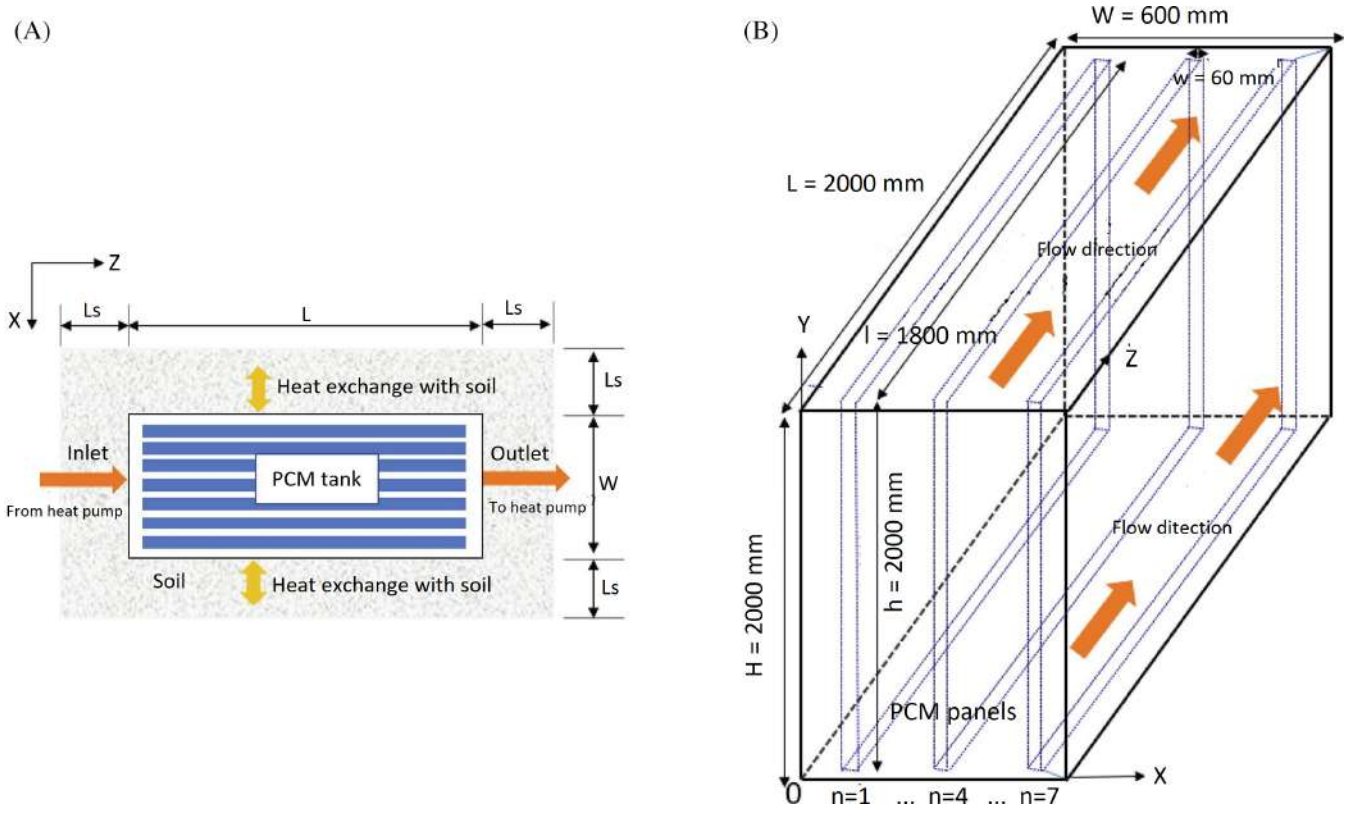

FIGURE 11 Schematic of buried water-PCM tank: (A) top view, (B) front-left view.[56] PCM, phase change material.

modes, respectively. The hybrid system designed for the underground shelter is demonstrated in Figure 13. MMWPT, GHEs, Water Loop HPs, water collectors, water separators, and pumps constitute the essential elements of the proposed system. The primary factors affecting performance in the emergency mode for the integrated system are the GHE length, MMWPT arrangement, and cooling water flow ratio. Table 9 is a list of the specific comparison criteria used in the study.[58]

- **Step 5:** The system's KPIs included effective discharge duration (EDD), the outlet temperature, and total emitted heat. Due to its effect on the energy efficiency of HP systems, the temperature drop (ΔT_{water}) during the EDD is a critical evaluation indicator.
- **Step 6:** A Taguchi design, also known as an orthogonal array, was designed for simulations after listing the parameters and their levels. A two-dimensional mathematical model was developed to simulate the processes of phase change and heat transfer within both the HTF and the soil medium surrounding the tank. A symmetrical boundary at the middle of the fourth panel is implemented to simplify the computational procedure.
- **Step 7:** The mathematical model is developed in MATLAB environment and validated through

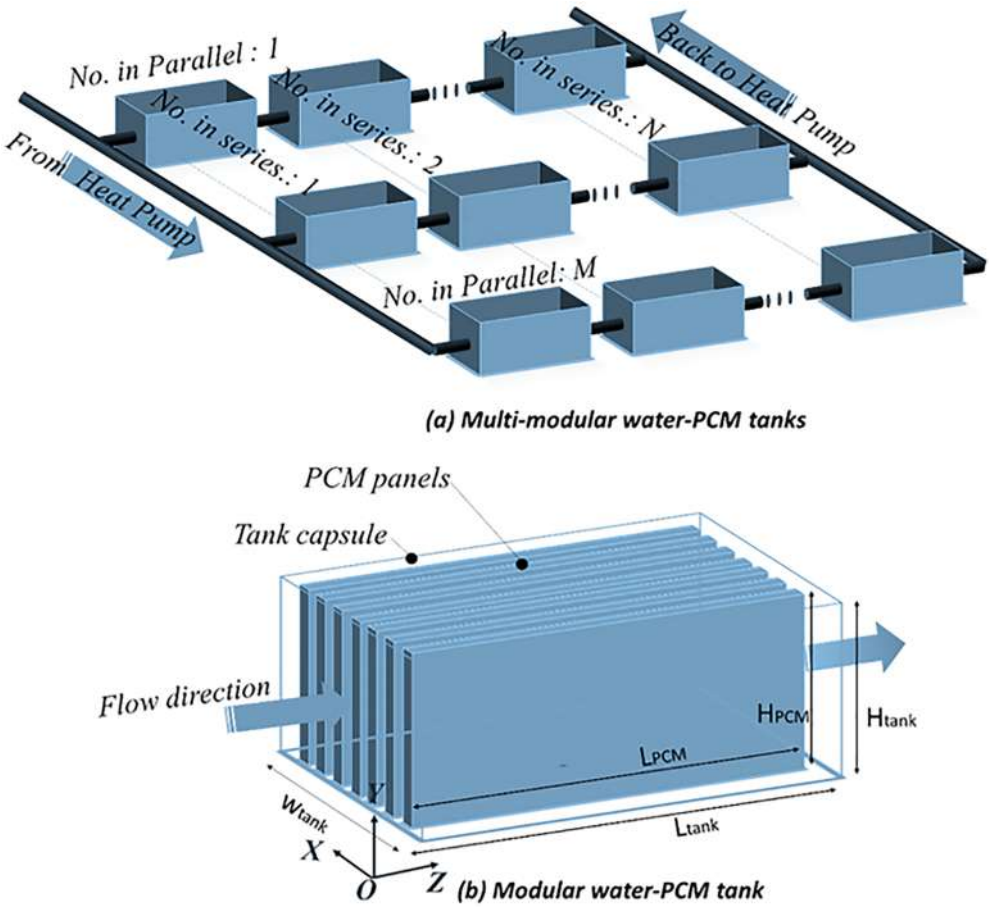

FIGURE 12 Schematic diagram of the multimodular water-PCM tanks.[57] PCM, phase change material.

experimentation, achieving a normalized mean bias error and root mean square error both below 10% and 30%, respectively. Subsequently, TRNSYS 18 is employed to interact with the data for simulation, with all parameter and level combinations specified as inputs in the MATLAB code. ANOVA was also used to assess the data and find out how each influential element varied and what influence it had. The reporting of factor ranking, and their primary influences was presented as an outcome. Subsequently, the appropriate combination of parameters is showcased.[59]

3.5.1 | Results and discussion on case study 3.5

The implementation of the recently planned buried water-PCM tank for load shifting is examined to use the system as a reference. Burying the water-PCM tank in the ground helps maintain the PCM in a solid state. The tank can offer latent thermal storage capacity in times of need. According to the findings, the underground water-PCM tank's cooling capacity is 24.96% greater than that of an insulated tank. Zeng et al[58] additionally investigate the effect of MMWPT configuration on the HP system's cooling performance. The outcome shows that the ΔT_{water} in the scenario with N (number of series tanks) $\times$ 5 (number of parallel tanks) is about four times as that with $N \times 1$. The related EDD, which is increased by dividing the water into five parallel water tanks, is 1.27 to 1.28 times longer. The ideal MMWPT matrix for the underground shelter is 3 $\times$ 5. In an emergency mode, MMWPT is expanded and scaled to serve as the GSHP's thermal storage system in an underground shelter. The hybrid system's thermo-economic performance in both normal and emergency modes are carried out. The average initial cost per unit EDD in emergency mode was found to be the most pertinent evaluation metric. Flowing ratio comes before GHE length and MMWPT matrix in the list of factors. The initial cost per unit EDD was dropped by 24.37% with the hybrid system's ideal design.

3.6 | Utilization of LHTES integrated with GSHP in office building

Peak load can be shifted using a GSHP integrated with a PCM cooling storage system, which is supposed to be both efficient and environmentally benign. In an office

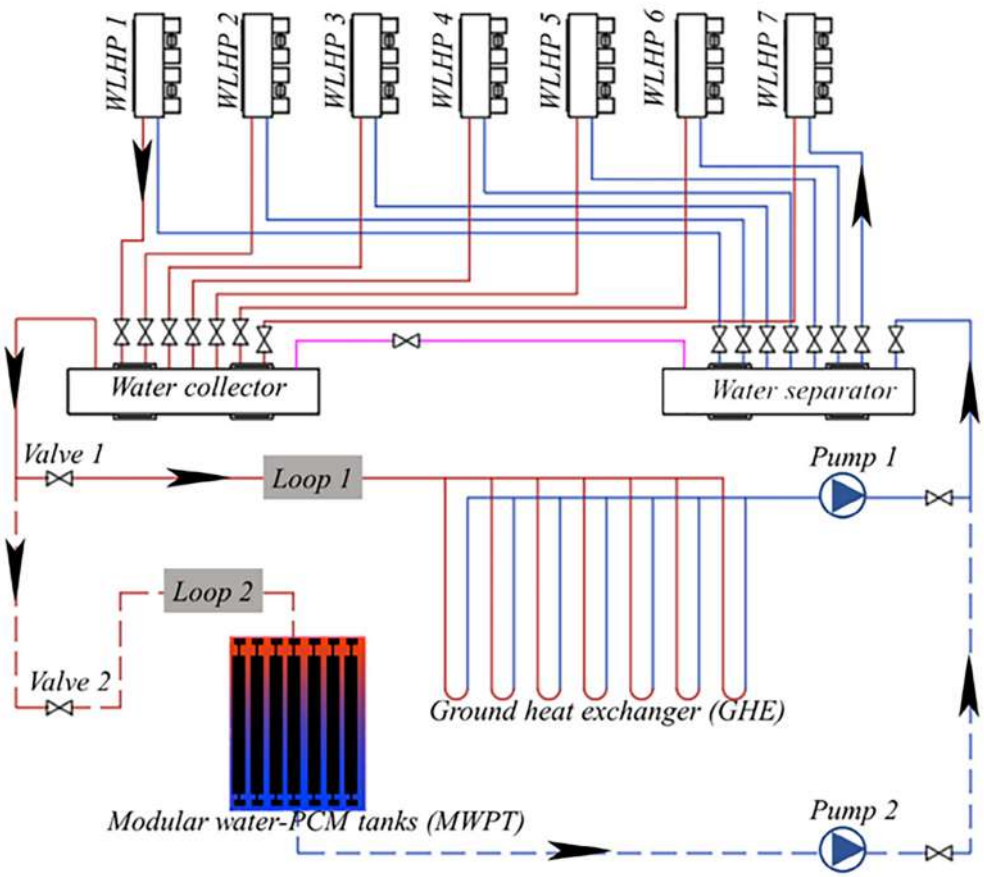

FIGURE 13 Schematic diagram of the hybrid system.[58]

TABLE 9 Values of variables used in the parametric study in the emergency mode.[58]

Variables	Base scenario	Values
GHE length(m)	2500	1800, 1900, 2000, 2100, 2200, 2300, 2400, 2500
MMWPT matrix	3 × 5	3 × 5, 3 × 4, 2 × 5
Cooling water flow ratio	2:8	0:10, 1:9, 2:8, 3:7, 4:6, 5:5

Abbreviations: GHE, geothermal heat exchanger; MMWPT, multimodular water phase change material tank.

block in Wuhan, China (30.52 N, 114.32 E), a GSHP system with a PCM cooling storage tank was the subject of this case study.

Both in the summer and the winter, the ground heat exchanger (GHX) is employed as a HEX. In the summer, PCM tanks are employed as cooling storage facilities. When a PCM needs to be charged cold at night in the summer, a cooling tower (CT) is employed as heat dissipation equipment. In the meantime, it serves as an additional heat dissipation device when the building cooling load exceeds the combined capacities of the GSHP and PCM tanks during the hot day. The integrated system's schematic is shown in Figure 14.

- **Step 1:** Operating modes of the system in various seasons are described as follows:
  - Summer: A CT removes heat while a GSHP unit charges the PCM tank with cold at night. The cold discharges during the day in two ways. First, the PCM tank supplies the cold, followed by the GSHP unit once the PCM tank has finished discharging. The leftover heat is dispersed by a CT if the building cooling load exceeds the combined capacity of the PCM tank and HP equipment. The chilled water is piped to the HP unit during the nighttime cold charging phase to be cooled to 4°C to 6°C before being supplied to the storage tank for heat exchange. When the water temperature drops below 8.3°C, the PCM freezes layer by layer. The 12°C water from the user's side is cooled to 9°C to 10°C in the cooling storage tank during the cooling discharge period in the daytime and is then chilled by a chiller to the desired 7°C.
  - Winter: The entire heating load is provided by the HP and the cold is exchanged in GHX.
  - Remaining seasons: The system ceases operation between March 1st and May 31st, as well as from October 1st to November 30th.

A numerical study was carried out on the office

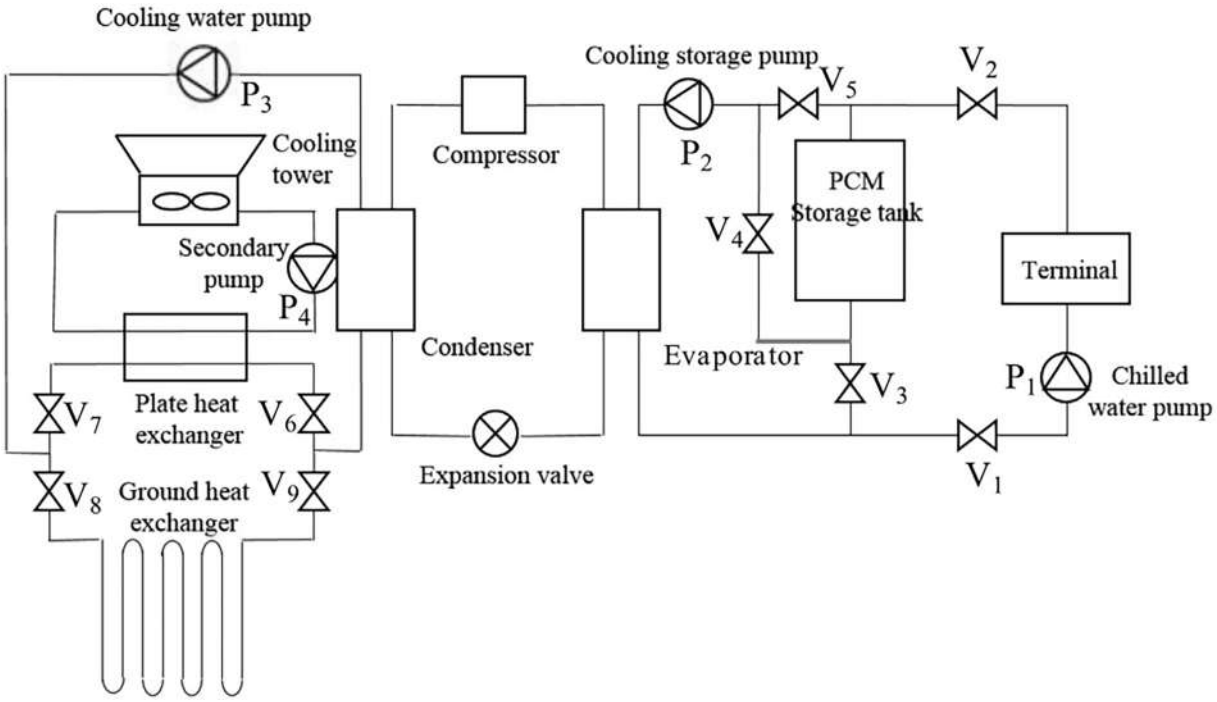

FIGURE 14 Schematic of combined system.[60]

building, focusing on a GSHP system integrated with a PCM cooling storage tank. This office building had a 5175 m^2 total area. During the summer, the cooling season extended from June 1 to September 30, while in the winter, it spanned from December 1 to February 28. In Table 10, the annual dynamic building load is displayed.

- **Step 2:** Both in the summer and the winter, ground heat exchangers (GHX) are employed for heat exchange. The overall length of GHX is determined by the office building's winter heating load. The GHX are single-*U*-shaped PE tubes. The borehole is 0.2 m in diameter, 100 m deep, and spaced 5 m apart. The tube has an internal diameter of 25 mm and an exterior diameter of 32 mm. Table 11 includes a list of the specific details of the latent heat storage tank.
- **Step 3:** The characteristics of the PCM storage tank are given in Table 11.
- **Step 4:** In cooling- or heating-dominated locations with a year-round imbalance in cooling and heating demands, the GSHP system requires connection to supplementary cooling/heating systems. An efficient way to deal with issues brought on by cooling and heating imbalance in various locations is to combine a GSHP with a TES system. The implementation of GSHP integrated with the PCM cooling storage system still faces a number of difficulties. The best way to operate this combination system for various buildings in various climates is challenging. Yet, there is currently insufficient study being done on integrated system optimization. As a result, the combined system is created in TRNSYS to perform system optimization.
- **Step 5:** The energy performance and economic analyses of the integrated system were investigated under different cooling storage ratios, representing the ratio of PCM cooling storage tank capacity to the total system cooling capacity. The optimal operational mode and cooling storage ratio for this combined system were identified.
- **Step 6:** A numerical model incorporating a GSHP connected to a PCM cooling storage system was created. The system's operation is simulated for a 20-year period under year-round continuous and intermittent conditions (with three designs) using the temperature difference control method of the CT.

TABLE 10 Annual dynamic building load.[60]

Load type	Value	Ratio of cooling load to heating load
Design cooling load(kW)	1045.46	2.42
Design heating load(kW)	432	
Cumulative cooling load(kWh)	682 695	3.6
Cumulative heating load(kWh)	189 132	

TABLE 11 Latent heat storage tank design parameters.

The size of tank	1.0 × 1.2 × 1.0 m
Heat loss coefficient, Ut	0.3 W/(m^2 K)
Total area of exchanger, Ahe	6 m^2
Coefficient of heat transfer, Uhe	150 W/(m^2 K)
Water volume in tank, Vw	0.45 m^3
PCM type	$CaCl_2 \cdot 6H_2O$
PCM enclosed size	140 × 120 × 70 mm
PCM total volume, Vpm	0.5 m^3
PCM melting point, Tm	29.9
PCM melting latent heat, L	187.49 kJ/kg
PCM density, ρpm	1710 kg/m^3
PCM specific heat, CPpm	1460 J/(kg K) (*s*) 2130 J/(kg K) (*l*)
PCM thermal conductivity, λpm	1.09 W/(m K) (*s*) 0.54 W/(m K) (*l*)

Abbreviation: PCM, phase change material.

- **Steps 7:** The model was developed in TRNSYS.

3.6.1 | Results and discussion on case study 3.6

The issue of soil heat accumulation can be efficiently solved by using GSHP in conjunction with a PCM cooling storage system, which also increases the HP unit's operational efficiency. A consistent operating performance and good energy efficiency were achieved by the GSHP with PCM cooling storage compared to that without. For this integrated system, the ideal mode of operation and cooling storage ratio were discovered. Based on numerical investigations, the optimal cooling storage ratio was determined to be 40%, taking into account both initial investment and operating costs. In comparison to the conventional GSHP hybrid CT system, the combined GSHP with PCM cooling storage system achieved a 34.2% reduction in the annual cost under a cooling storage ratio of 40%. The PCM cooling storage system employed partial cooling storage and cooling storage before modes. In comparison to a typical GSHP hybrid CT system without cooling storage, the operational mode could effectively release the stored cooling energy, thereby enhancing the efficiency of cooling storage utilization and reducing operational costs. A key element in the combined system's ideal design and functioning is the cooling storage ratio. Varying cooling storage ratios have an impact on the combined system's operation energy performance and economy. Nevertheless, factors such as building type, location, and system utilization mode impact the optimal cooling storage ratio. This scenario illustrates an instance of the optimum utilization of the combined system. The optimal design can contribute to enhancing both theoretical and practical insights into integrated systems, enabling broader applications of such systems.

3.7 | Utilization of LHTES integrated with solar energy system in Tibet

An established engineering approach to address the disparity between the heat demand of a given building and the heat supply from a solar heating system (SHS) involves incorporating latent heat energy storage. Zeng et al[58] explored a SHS integrated with PCM specifically designed for Tibet. This system is notable for its adaptability to factors such as high altitude, solar radiation, air pressure, and water boiling temperature, among others. The entire procedure involves: (1) recognizing the unique features of Tibet's climate and altitude, along with the specific demands for the solar system; (2) creating a SHS integrated with PCM, based on a selected building in Lhasa and devising applicable control strategies; (3) evaluating the energy performance of the system across various operational scenarios; and (4) suggesting the most appropriate operational scheme and design strategy for the system.

- **Step 1:** The case study building in Lhasa has five stories; each has a heating area of 3778.87 m^2 and a height of 3.9 m. The building's hourly heating load (from November 4th to March 19th of the subsequent year) is computed using DEST software. The heating system's supply water temperature and return water temperature are determined through load value calculations. The timeframe for the SHS-PCM numerical models encompasses the entire heating season, spanning from November to March.
- **Step 2:** The minimum solar portion for building heating should be 60%, according to the Technical Code for SHSs (GB 50495-2009).[61] The roof space of a building, however, limits the overall area of solar heat collectors. Two rows with 44 collector panels each are finally chosen, taking into account the need for the edge wall shelter and maintenance area. The PCM storage tank is considered solely as latent heat storage, adhering to the heat storage capacity specified in GB 50495-2009.[61] Table 12 displays the selected parameters for both tanks.[62]
- **Step 3:** To meet the temperature specifications of the heating system, a paraffinic PCM with a phase change temperature ranging from 40°C to 80°C was considered.

- **Step 4:** The authors have proposed a conceptual design for the PCM-integrated SHS (SHS-PCM) to align with the heat load and demand of the targeted building. Figure 15 illustrates the system, which comprises a solar collecting system (SCS), a phase change thermal storage system (PCTSS), and an indoor heating system. The SCS incorporates flat plate solar thermal collectors (FSTCs), a plate HEX, pump 1, valves, pipelines, and other components as the primary heat source. Serving as an additional heat source, the PCTSS includes a PCM storage tank, an assistance heat source (AHS), a plate HEX, pump 2, valves, pipelines, and other elements.[64]
- **Step 5:** The heating conditions, solar energy contribution rate, and overall heating system energy-saving capabilities are examined using a public building in Lhasa as the research target. This analysis is done using various PCM storage tanks and various terminal shapes. For the entire heating season, a control strategy and numerical models were developed for each of the seven specific operation modes, as outlined in Table 13. The seven suggested operation modes are as follows:
  - Mode 1: free cooling.
  - Mode 2: preservation of the heat absorbed by the solar collector in the PCM storage tank during periods of no heating demand.
  - Mode 3: direct supply of the heating demand through the solar collector.
  - Mode 4: utilization of the heat absorbed by the solar collector to fulfill heating demands, storing any excess heat in the PCM storage tank.
  - Mode 5: utilization of the heat stored in the PCM storage tank to fulfill the heating demands.
  - Mode 6: utilization of both the heat stored in the PCM storage tank and auxiliary heating sources to fulfill the heating demands.
  - Mode 7: sole reliance on auxiliary heat sources to meet the heating demands. Mathematical models were developed for each of the seven operation

TABLE 12 Selection parameters for ordinary water tank and PCM storage tank.[62]

	Nomenclature	Units	Ordinary water tank	PCM storage tank
Heat storage capacity	Q_m	GJ	0.63	0.63
Volume of tank	V_{hp}	m^3	3 × 2.5 × 4	3 × 2.5 × 0.8
Volume PCM plate	V_{pp}	m^3	—	3 × 2.5 × 0.08
Number of PCM plates	N_{pp}		—	6
PCM materials				Paraffin
Phase-transition temperature	T_m	°C	—	47
Terminal form			fan coil	Fan coil
Supply and return heating temperature	$T_{e,in}/T_{e,o}$	°C	45/40	45/40

Abbreviation: PCM, phase change material.

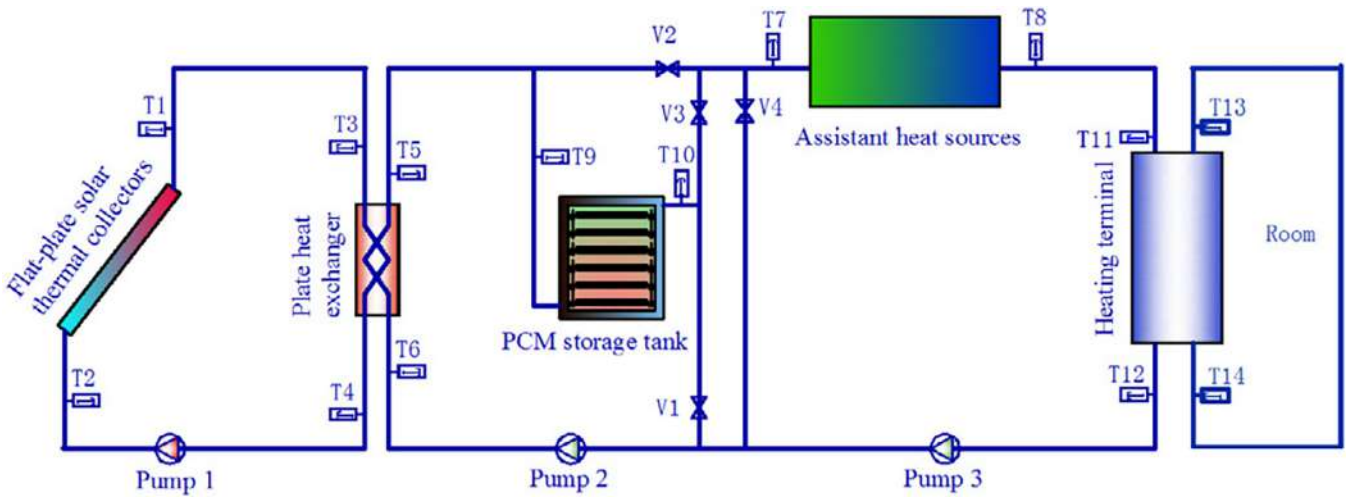

FIGURE 15 Schematic diagram of the SHS-PCM.[63] PCM, phase change material; SHS, solar heating system.

TABLE 13 Operating modes and control parameters of the SHS-PCM.[62]

Mode	Detail	Flat-plate solar collector	PCM storage tank	Auxiliary heat source (AHS)	Operation
Mode 1	Natural cooling	Off	Off	Off	All valves closed
Mode 2	FSTC for PCM storage tank	On	On	Off	Valves V7 and V1 opened; pumps 1 and 2 on
Mode 3	FSTC for indoor heating	On	Off	Off	Valves V7, V2, V6, and V5 opened; pumps 1 and 2 on
Mode 4	FSTC for PCM storage tank and indoor heating	On	On	Off	Valves V7, V1, V2, V6, and V5 opened; pumps 1 and 2 on
Mode 5	PCM storage tank for indoor heating	Off	On	Off	Valves V3, V6, V5, and V4 opened; pump 2 on
Mode 6	PCM storage tank and AHS for indoor heating	Off	On	On	Valves V3, V6, V5, V4 opened; pump 2 on; AHS on
Mode 7	AHS for indoor heating	Off	Off	On	Valves V6, V5, V4, and V2 opened; pump 2 on; AHS on

Abbreviations: AHS, assistance heat source; FSTC, flat plate solar thermal collector; PCM, phase change material; SHS, solar heating system.

modes mentioned above, considering the impact of outdoor meteorological parameters and terminal load on the heating system.

Concerning the valve and temperature designations depicted in Figure 15, the system's operating modes and control parameters are detailed in Table 13.

- **Step 6:** Design parameters, meteorological data, and hourly heating load were input into MATLAB as the known conditions and the time step was set to 20 minutes, aligning with the numerical models of a SHS coupled with a PCM-based TES system developed in MATLAB. Computed dynamic properties of the performance indices of the AHS, PCM storage tank, and FSTCs during the heating process include operation time for each mode, fluid inlet and outlet temperatures, heating quantity from auxiliary heat sources, phase change ratio, and thermal efficiency of solar collectors. A novel dynamic simulation model for energy performance, namely, the Department of Housing and Urban-Rural in Tibet, was employed to analyze the energy efficiency of both the building and the connected SHS. This analysis was conducted under three operational schemes and two distinct heating selections. Based on these assessments, optimal models and operational patterns were chosen.
- **Step 7:** The model was developed in MATLAB.

3.7.1 | Results and discussion on case study 3.7

According to the findings, a SHS with a PCM tank offers a 34% greater capacity for energy savings than a conventional water tank heating system. Regarding the energy efficiency of the system, daytime heating surpasses full-day heating. It is recommended to select design parameters for the PCM storage tank that provide a daily heat storage capacity covering 70% to 80% of the heating season. The maximum energy savings are achieved with a floor radiant system having supply and return water temperatures of 40°C and 35°C, respectively. The real-time parameters for the entire heating season, considering various operation modes of the system, can be acquired by solving the simulation models. These parameters serve as a reference for optimizing the design and operation of the actual system.

4 | DISCUSSION AND CONCLUSIONS

TES is a proven technology to increase the energy efficiency of buildings in several ways, for example, by increasing the share of renewable energy use or by increasing the efficiency of heating and cooling systems in buildings. A proper design of TES can be a challenging and sophisticated task, considering the wide range of existing and emerging technologies for TES as well as the variety of building applications requiring the integration of TES. Hence, an optimal design of TES system has increasingly attracted the attention of researchers and is a subject of many recent studies. In this context, a systematic design methodology for TES that can be adapted to a range of applications is beneficial, easing the design procedure, thus removing the barrier for deployment of TES systems in practice. However,

TABLE 14 Summary of designed information for the seven case studies.

	Objective	Inputs/constraints	Design	Output
Case 1	• Thermal comfort	• Heat flow rates • Comfort zone limit • Technology: PCM	*Parameters*: • Viable charging and discharging • Thickness of the floor • Thickness of the slab • Thickness of earthbag block • Area of Earthbag block • Area of Earthbag wall *KPIs*: • The inner surface temperature reduction • The viable PCM charging and discharging duration *Optimization method and tools*: • Genetic Algorithm (GA)/ MATLAB	• Optimal thickness of earthbag wall • Optimal thickness of the selected PCMs • Optimal building orientation
Case 2	• Seasonal performance • Cost	• Mass flow rate of HTF • Thermal demand and resource availability curves derived from a detailed dynamic simulation • Available space for installation of the tanks • Technology: indirect-contact TES, water tank and borehole	*Parameters*: • Upper and lower working temperatures • Number of solar thermal collectors • Number of geothermal boreholes • Depth of boreholes • Volume of the integration storage per solar collectors' area • Volume of the gray water storage • Surface of the solar heat exchanger serpentine in the integration storage • Surface of the gray water heat exchanger serpentine in the integration storage • Surface of the heat exchanger serpentine in the gray water storage *KPIs*: • Global cost of the system within its estimated lifecycle (30 years) • Seasonal performance factor *Optimization method and tools*: Metaheuristic population-based PSO algorithm/GenOpt and TRNSYS	• Optimal size of solar loop • Optimal size of exhaust DHW storage • Optimal number of boreholes • Optimal recharging strategy for ground field
Case 3	• Energy efficiency • Thermal comfort • Cost • Energy flexibility	• Cooling load • The nominal, minimum and maximum water flow rates • The nominal lower and upper temperature of the water • Defined comfort limits • Technology: PCM	*Parameters*: • Charging and discharging time • Ceiling panel dimensions • PCM thickness • Number of ceiling panel *KPIs*: • Global cost • Payback period	• Optimal discharge method (water vs, air-based system) • Optimal water circulation schedule and control • Optimal water supply temperature • Optimal water flow rate

(Continues)

TABLE 14 (Continued)

	Objective	Inputs/constraints	Design	Output
		• Limit on the volume of PCM per panel • Available ceiling area	• Operative temperature • Vertical temperature difference • Specific cooling power • Energy use • Supply water temperature *Optimization method and tools*: Parametric analysis and laboratory experiment/TRNSYS	• Optimal airflow rate (night ventilation)
Case 4	• Levelized cost of energy	• The hot and cold tank temperatures • Building load demand • Technoeconomic and environmental data of each component in the hybrid system • Sizing variable boundaries • Technology: water tank	*Parameters*: • Capacity of TES • Charging/discharging time • Power capacity of compressor/turbine train • Maximum pressure of air storage tank (AST) • Volume of AST • Number of installed PV panels *KPIs*: • Levelized cost of energy (LCOE) • Building self-sufficiency (SSR) • Heat recovery ratio (HHR) • Round-trip efficiency (RTE) *Optimization method and tools*: PSO algorithm/MATLAB	• Optimal TES capacity and plant configuration
Case 5	• Peak load shifting	• Peak load in peacetime and emergency time • Technology: water-PCM tank	*Parameters*: • Arrangement and dimensions of the water-PCM tank • Arrangement and dimensions of PCM panels inside the tank • HTF's velocity • GHE length • Cooling water flow ratio *KPIs*: • Outlet temperature • Effective discharge duration (EDD) • Total heat emitted • Temperature drop during EDD *Optimization method and tools*: Parametric study/MATLAB and TRNSYS	• Optimal MMWPT arrangement
Case 6	• Energy performance • Cost	• Design cooling load • Design heating load • Cumulative cooling load • Cumulative heating load • Water temperature • Total area • Technology: PCM	*Parameters*: • Size of the tank • Water volume in the tank • PCM total volume • PCM enclosed size • Total area of exchanger • Setting temperature to stop charging (PCM) *KPIs*: • Initial investment • Operating cost • Energy used Optimization method and tools:	• Optimal operation mode • Optimal cooling storage ratio

TABLE 14 (Continued)

	Objective	Inputs/constraints	Design	Output
			Numerical analyses/TRNSYS	
Case 7	• Energy flexibility	• Heating area • Building's hourly heating load • Technology: PCM • Solar portion for building heating	*Parameters*: • Heat storage capacity • Dimensions of water tank • Dimensions of PCM tank • Annual heating load • Setting temperature to stop charging (PCM) *KPIs*: • Solar energy contribution rate • Energy-saving Optimization method and tools: Numerical analyses/MATLAB	• Optimal operation mode • Optimal supply water temperature • Optimal return water temperature

few studies have been yet devoted to this topic. To support the establishment of a systematic design methodology, the current study has introduced the essential steps that should be taken for the optimal design of TES systems as follows.

Characterization of the thermal process is the first step that should be taken in designing TES systems. Often, three parameters related to the HTF can be used for this purpose, namely the upper temperature, the lower temperature, and the flow rate. Likewise, a detailed information on the thermal resources and thermal demands should be available. This information can identify the main system design parameters which are the charging time, discharging time and the storage capacity. Considering the process and system boundaries, at this stage it is possible to specify the storage characteristics that can best suit to the application. Afterwards, in addition to the parameters related to the TES system itself, the parameters related to the integration of the system to building should also be specified in the next design step. In a smart design scheme, the aim is to optimize the system operational performance, either considering merely the TES system or the storage system in conjunction with the rest of the plant, that is, where it is integrated. Hence, relevant application-specific KPIs will be defined for performance evaluation following by defining the optimization methodology and tools employed for this purpose in the next design steps. Finally, the robustness of the design should be tested using available techniques, for example, sensitivity analysis. After this step, the design parameters may be refined in some design iterations if needed.

The introduced design steps have been applied to seven different case studies, namely design of:

1. Earthbag-PCM integrated walls to maximize thermal comfort in temporary housings.
2. Geothermal borehole and water tank storage systems to maximize seasonal performance factor and minimize the global lifecycle cost of solar-assisted GHPS in a restaurant.
3. TABS including ceiling panel with PCM material embedded with water pipe to optimize energy efficiency, thermal comfort, cost, and flexibility in a test room at a university campus.
4. A water tank storage in conjunction with a conventional air energy storage to minimize the levelized cost of energy while achieving maximum building self-sufficiency in integrated energy systems.
5. An underground water-PCM tank to optimize a HP cooling performance in an underground shelter.
6. A PCM cooling storage tank to optimize the energy performance and cost of a GSHP system in an office building.
7. A PCM storage tank integrated with a SHS to optimize solar energy contribution rate, and overall heating system energy-saving in a public building.

Following Section 3, Table 14 summarizes the information obtained from the design procedure of the above case studies considering the proposed design steps. As can be seen, there is a wide diversity among the design cases in terms of design objective, input, design, and output parameters. Particularly, the design parameters, which include both the system and integration parameters, can be quite different from one application to another. However, despite this diversity which include both sensible and latent TES employed in different types of buildings, it can be concluded that the design procedure in all of them can be broken down into the introduced design steps as explained in Section 3, except step 8 that has been omitted in all case studies due to lack of information regarding the robustness of the design procedure.

All above case studies in the current research are related to retrofit applications. Following this work, it is recommended to evaluate the design methodology with applying it to greenfield applications. It is expected that the application of the proposed design methodology is more straightforward for greenfield application though. Moreover, thermo-chemical storage system is not among the case studies and the design process of such storage needs further investigation. The proposed design methodology is an attempt to give a structure to the design of TES systems. While the proposed design steps can be adapted according to chosen storage technology, they can be considered as a general base to develop a more systematic methodology for the design of TES systems in future works.

ACKNOWLEDGEMENTS

This research work was conducted as part of IEA ECES Annex 37 "Smart Design and Control of Energy Storage." This work is financially supported by Energy Technology Development and Demonstration Programme (EUDP), a funding scheme under the Danish Energy Agency with project no. 64020-2106.

CONFLICT OF INTEREST STATEMENT

The authors declare the following financial interests/personal relationships which may be considered as potential competing interests: financial support was provided by Energy Technology Development and Demonstration Programme (EUDP), a funding scheme under the Danish Energy Agency with Project No. 64020-2106.

DATA AVAILABILITY STATEMENT

The data that support the findings of this study are available from the corresponding author upon reasonable request.

ORCID

Samira Rahnama https://orcid.org/0000-0002-5273-524X

REFERENCES

1. Lucon O, Ürge-Vorsatz D, Ahmed AZ, et al, 2014. *Buildings*. Cambridge, UK and New York, NY: Cambridge University Press.
2. González-Torres M, Pérez-Lombard L, Coronel JF, Maestre IR, Yan D. A review on buildings energy information: trends, end-uses, fuels and drivers. *Energy Rep*. 2022;8:626-637.
3. Sharma A, Tyagi VV, Chen CR, Buddhi D. Review on thermal energy storage with phase change materials and applications. *Renew Sustain Energy Rev*. 2009;13(2):318-345.
4. Violidakis I, Atsonios K, Iliadis P, Nikolopoulos N. Dynamic modeling and energy analysis of renewable heating and electricity systems at residential buildings using phase change material based heat storage technologies. *J Energy Storage*. 2020;32:101942.
5. Dincer I, Rosen MA. *Thermal Energy Storage: Systems and Applications*. West Sussex, UK: John Wiley & Sons; 2021.
6. Dheep GR, Sreekumar A. Influence of nanomaterials on properties of latent heat solar thermal energy storage materials—a review. *Energy Convers Manag*. 2014;83:133-148.
7. Alva G, Lin Y, Fang G. An overview of thermal energy storage systems. *Energy*. 2018;144:341-378.
8. Navarro L, De Gracia A, Colclough S, et al. Thermal energy storage in building integrated thermal systems: a review. Part 1. Active storage systems. *Renew Energy*. 2016;88:526-547.
9. Navarro L, De Gracia A, Niall D, et al. Thermal energy storage in building integrated thermal systems: a review. Part 2. Integration as passive system. *Renew. Energy*. 2016;85:1334-1356.
10. Heier J, Bales C, Martin V. Combining thermal energy storage with buildings—a review. *Renew Sustain Energy Rev*. 2015;42:1305-1325.
11. Kuravi S, Trahan J, Goswami DY, Rahman MM, Stefanakos EK. Thermal energy storage technologies and systems for concentrating solar power plants. *Prog Energy Combust Sci*. 2013;39(4):285-319.
12. Gibb D, Johnson M, Romaní J, Gasia J, Cabeza LF, Seitz A. Process integration of thermal energy storage systems—evaluation methodology and case studies. *Appl Energy*. 2018;230:750-760.
13. Zheng N, Wirtz RA. A hybrid thermal energy storage device, part 1: design methodology. *J Electron Packag*. 2004;126(1):1-7.
14. Li Y, Ding Z, Shakerin M, Zhang N. A multi-objective optimal design method for thermal energy storage systems with PCM: a case study for outdoor swimming pool heating application. *J Energy Storage*. 2020;29:101371.
15. Alam M, Devapriya S, Sanjayan J. Experimental investigation of the impact of design and control parameters of water-based active phase change materials system on thermal energy storage. *Energ Buildings*. 2022;268:112226.
16. Ručevskis S, Akishin P, Korjakins A. Parametric analysis and design optimisation of PCM thermal energy storage system for space cooling of buildings. *Energ Buildings*. 2020;224:110288.
17. Cui B, Gao DC, Xiao F, Wang S. Model-based optimal design of active cool thermal energy storage for maximal life-cycle cost saving from demand management in commercial buildings. *Appl Energy*. 2017;201:382-396.
18. Maleki H, Ashrafi M, Ilghani NZ, Goodarzi M, Muhammad T. Pareto optimal design of a finned latent heat thermal energy storage unit using a novel hybrid technique. *J Energy Storage*. 2021;44:103310.
19. Kalbande VP, Fating G, Mohan M, Rambhad K, Sinha AK. Experimental and theoretical study for suitability of hybrid nano enhanced phase change material for thermal energy storage applications. *J Energy Storage*. 2022;51:104431.
20. Kalbande VP, Walke PV, Rambhad K. Performance of oil-based thermal storage system with parabolic trough solar collector using Al_2O_3 and soybean oil nanofluid. *Int J Energy Res*. 2021;45:15338-15359.
21. Nandanwar YN, Kalbande VP, Mohan M, Rambhad K, Walke PV. An approach toward higher electrical conversion efficiency of solar photovoltaic module using phase change materials. *Energy Storage*. 2022;4(6):e379.

22. Bastien D, Athienitis AK. Passive thermal energy storage, part 1: design concepts and metrics. *Renew Energy*. 2018;115:1319-1327.
23. Bastien D, Athienitis AK. Passive thermal energy storage, part 2: design methodology for solaria and greenhouses. *Renew Energy*. 2017;103:537-560.
24. Chen Y, Galal KE, Athienitis AK. Design and operation methodology for active building-integrated thermal energy storage systems. *Energ Build*. 2014;84:575-585.
25. Pirasaci T, Wickramaratne C, Moloney F, Goswami DY, Stefanakos E. Influence of design on performance of a latent heat storage system at high temperatures. *Appl Energy*. 2018;224:220-229.
26. Deng S, Nie C, Jiang H, Ye WB. Evaluation and optimization of thermal performance for a finned double tube latent heat thermal energy storage. *Int J Heat Mass Transf*. 2019;130:532-544.
27. Raul A, Jain M, Gaikwad S, Saha SK. Modelling and experimental study of latent heat thermal energy storage with encapsulated PCMs for solar thermal applications. *Appl Therm Eng*. 2018;143:415-428.
28. Metin C, Hacipasaoglu SG, Alptekin E, Ezan MA. Implementation of enhanced thermal conductivity approach to an LHTES system with in-line spherical capsules. *Energy Storage*. 2019;1(1):e39.
29. Hübner S, Eck M, Stiller C, Seitz M. Techno-economic heat transfer optimization of large scale latent heat energy storage systems in solar thermal power plants. *Appl Therm Eng*. 2016;98:483-491.
30. Lin W, Ma Z, Ren H, Gschwander S, Wang S. Multi-objective optimisation of thermal energy storage using phase change materials for solar air systems. *Renew Energy*. 2019;130:1116-1129.
31. Yuksel YE, Ozturk M, Dincer I. Performance assessment of a solar tower-based multigeneration system with thermal energy storage. *Energy Storage*. 2019;1(4):e71.
32. Campos-Celador Á, Diarce G, Larrinaga P, García-Romero AM. A simple method for the design of thermal energy storage systems. *Energy Storage*. 2020;2(6):e140.
33. IRENA. *Innovation Outlook: Thermal Energy Storage*. Abu Dhabi: International Renewable Energy Agency; 2020.
34. Guo X, Goumba AP, Wang C. Comparison of direct and indirect active thermal energy storage strategies for large-scale solar heating systems. *Energies*. 2019;12(10):1948. doi:10.3390/en12101948
35. Gibb D, Seitz A, Johnson M, et al. *Applications of Thermal Energy Storage in the Energy Transition—Benchmarks and Developments* . IEA Technology Collaboration Programme on Energy Conservation through Energy Storage (IEA-ECES Annex 30). Trondheim, Norway: SINTEF Energy Research; 2018.
36. Cabeza LF, Galindo E, Prieto C, Barreneche C, Fernández AI. Key performance indicators in thermal energy storage: survey and assessment. *Renew Energy*. 2015;83:820-827. doi:10.1016/j.renene.2015.05.019
37. Cabeza LF, Borri E, Gasa G, Zsembinzski G, Lopez-Roman A, Prieto C. *Definition of Key Performance Indicators (KPIs) to Evaluate Innovative Storage Systems in Concentrating Solar Power (CSP) Plants*. International Solar Energy Society, Freiburg, Germany; Virtual Congress. 2021.
38. Giacone E, Mancò S. Energy efficiency measurement in industrial processes. *Energy*. 2012;38(1):331-345.
39. dos Santos DM, Beirão JNDC. Generative tool to support architectural design decision of earthbag building domes. Paper presented at: XXI Congreso Internacional de la Sociedad Iberoamericana de Gráfica Digital; November. 2017: 538-543. doi:10.5151/sigradi2017-083
40. Ross BE, Willis M, Datin P, Scott R. Wind load test of earthbag wall. *Buildings*. 2013;3:532-544. doi:10.3390/buildings3030532
41. Ali S, Martinson B, Al-Maiyah S. Evaluating neutral, preferred, and comfort range temperatures and computing adaptive equation for Kano region computing adaptive equation for Kano region. 2020.
42. Batagarawa A. *Assessing the Thermal Performance of Phase Change Materials in Composite Hot Humid/Hot Dry Climates: an Examination of Office Buildings in Abuja-Nigeria*; 2013. PhD thesis. Newcastle University.
43. Ferrara M, Fabrizio E. Optimized design and integration of energy storage in solar-assisted ground-source heat pump systems. *Build Simul*. 2023, under publication.;16:1933-1948.
44. Biglia A, Ferrara M, Fabrizio E. On the real performance of groundwater heat pumps: experimental evidence from a residential district. *Appl Therm Eng*. 2021;192:116887.
45. Ferrara M, Dabbene F, Fabrizio E. Optimization algorithms supporting the cost-optimal analysis: the behavior of PSO. *Building Simulation 2017*. Vol 15. San Francisco, CA: IBPSA; 2017:1418-1427.
46. Bogatu DI, Kazanci OB, Olesen BW. An experimental study of the active cooling performance of a novel radiant ceiling panel containing phase change material (PCM). *Energy Build*. 2021;243:110981. doi:10.1016/j.enbuild.2021.110981
47. Bogatu D-I, Allerhand JQ, Kazanci OB, Olesen BW. D6.3 Report on the usability of TABS panels (radiant ceiling panels with PCM), HybridGEOTABS. 2019.
48. Allerhand JQ, Kazanci OB, Olesen BW. Investigation of the influence of operation conditions on the discharge of PCM ceiling panels. *E3S Web Conf*. 2019;111:3-9. doi:10.1051/e3sconf/201911103021
49. Allerhand JQ, Kazanci OB, Olesen BW. Energy and thermal comfort performance evaluation of PCM ceiling panels for cooling a renovated office room. *E3S Web Conf*. 2019;111:03020. doi:10.1051/e3sconf/201911103020
50. Zhang C, Kazanci OB, Levinson R, et al. Resilient cooling strategies—a critical review and qualitative assessment. *Energy Build*. 2021;251:111312. doi:10.1016/j.enbuild.2021.111312
51. Bergia Boccardo L, Kazanci OB, Quesada Allerhand J, Olesen BW. Economic comparison of TABS, PCM ceiling panels and all-air systems for cooling offices. *Energy Build*. 2019;205:109527. doi:10.1016/j.enbuild.2019.109527
52. Bazdar E, Sameti M, Nasiri F, Haghighat F. Compressed air energy storage in integrated energy systems: a review. *Renew Sustain Energy RevRenew Sustain Energy Rev*. 2022;167:112701. doi:10.1016/j.rser.2022.112701
53. Ortega-Fernández I, Zavattoni SA, Rodríguez-Aseguinolaza J, D'Aguanno B, Barbato MC. Analysis of an integrated packed bed thermal energy storage system for heat recovery in compressed air energy storage technology. *Appl EnergyAppl Energy*. 2017;205:280-293. doi:10.1016/j.apenergy.2017.07.039
54. Bazdar E, Fuzhan N, Fariborz H. *Effect of low-temperature thermal energy storage on the hybrid PV-compressed air energy*

storage operation. 8th World Conference on Photovoltaic Energy Conversion EFFECT; Milan, Italy. 2022:1609-1616. doi: 10.4229/WCPEC-82022-5DV.2.19

55. Bazdar E, Nasiri F, Haghighat F. Optimal planning and configuration of adiabatic-compressed air energy storage for urban buildings application: techno-economic and environmental assessment. *J Energy Storage*. 2024;76:109720.
56. Zeng C, Cao X, Haghighat F, et al. Buried water-phase change material storage for load shifting: a parametric study. *Energ Buildings*. 2020;227:110428.
57. Zeng C, Yuan Y, Cao X, et al. Operating performance of multi-modular water-phase change material tanks for emergency cooling in an underground shelter. *Int J Energy Res*. 2022;46(4): 4609-4629.
58. Zeng C, Yuan Y, Haghighat F, et al. Thermo-economic analysis of geothermal heat pump system integrated with multi-modular water-phase change material tanks for underground space cooling applications. *J Energy Storage*. 2022;45:103726.
59. Gao X, Zhang Z, Yuan Y, Cao X, Zeng C, Yan D. Coupled cooling method for multiple latent heat thermal storage devices combined with pre-cooling of envelope: model development and operation optimization. *Energy*. 2018;159:508-524.
60. Zhu N, Hu P, Lei Y, Jiang Z, Lei F. Numerical study on GSHP integrated with phase change material cooling storage system in office building. *Appl Therm Eng*. 2015;87: 615-623.
61. Ministry of Housing and Urban-Rural Development of the People's Republic of China. *Technical Code for Solar Heating System*. Beijing, China: China Architecture & Building Press; 2009.
62. Zhao J, Ji Y, Yuan Y, Zhang Z, Lu J. Energy-saving analysis of solar heating system with PCM storage tank. *Energies*. 2018; 11(1):237.
63. Zhao J, Ji Y, Yuan Y, Zhang Z, Lu J. Seven operation modes and simulation models of solar heating system with PCM storage tank. *Energies*. 2017;10(12):2128.
64. Zhao J, Yuan Y, Haghighat F, Lu J, Feng G. Investigation of energy performance and operational schemes of a Tibet-focused PCM-integrated solar heating system employing a dynamic energy simulation model. *Energy*. 2019;172:141-154.

How to cite this article: Rahnama S, Khatibi M, Maccarini A, et al. A methodical approach for the design of thermal energy storage systems in buildings: An eight-step methodology. *Energy Storage*. 2024;6(2):e600. doi:10.1002/est2.600